APPENDIX E

Underwater Sound Propagation Assessment (JASCO 2017)

This page has been intentionally left blank for double-sided printing

Underwater Sound Propagation Assessment

Nexen Energy ULC Flemish Pass Exploration Drilling Project (2018–2028)

Submitted to:

Steve Bonnell
AMEC Foster Wheeler
Project number: TF1693501

Authors:

Marie-Noël Matthews
Zahraalsadat Alavizadeh
Loren Horwich
Mikhail Zykov

6 February 2018

P001401-001
Document 01514
Version 2.0

JASCO Applied Sciences (Canada) Ltd
Suite 202, 32 Troop Ave.
Dartmouth, NS B3B 1Z1 Canada
Tel: +1-902-405-3336
Fax: +1-902-405-3337
www.jasco.com

Suggested citation:

Matthews M.-N. R., Z. Alavizadeh, L. Horwich, and M. Zykov. 2017. *Underwater Sound Propagation Assessment: Nexen Energy ULC Flemish Pass Exploration Drilling Project (2018–2028)*. Document 01514, Version 2.0. Technical report by JASCO Applied Sciences for AMEC Foster Wheeler.

Disclaimer:

The results presented herein are relevant within the specific context described in this report. They could be misinterpreted if not considered in the light of all the information contained in this report. Accordingly, if information from this report is used in documents released to the public or to regulatory bodies, such documents must clearly cite the original report, which shall be made readily available to the recipients in integral and unedited form.

Table of Contents

Figures

Tables

1. Introduction

Nexen Energy ULC (Nexen) is planning an 11-year exploration drilling program off eastern Newfoundland, from 2018 to 2028. AMEC Foster Wheeler (AMEC) have been contracted to produce an environmental assessment for this project. JASCO Applied Sciences (JASCO) conducted a modelling study to estimate distances to underwater sound level thresholds associated with injury and disturbance to marine life during planned operations. Operations are planned to occur in the Exploration Licenses (EL) 1144 and 1150, in the Flemish Pass region (Figure 1). Operations may include the use of drill ships, a semi-submersible drilling platform, supply vessels, and a Vertical Seismic Profiler (VSP) airgun array.

For this study, JASCO modelled two scenarios: operation of a VSP airgun array, and operation of a drilling platform that was defined as a semi-submersible platform with a supply vessel alongside. These scenarios provide conservative estimates of the distances to marine mammal impact thresholds for the various activities expected to occur during the Nexen Energy ULC Flemish Pass Exploration Drilling Project (the Project). Each scenario was modelled at two locations: a shallow (378 m) site in EL 1150 and a deep (1137 m) site in EL 1144.

The underwater acoustic signature of the VSP airgun array was predicted with a specialized computer model that accounts for individual airgun volumes and the array geometry. Source levels from the semi-submersible and the supply vessel were predicted based on frequency-dependent levels for cavitating propellers, adjusted for the characteristics of the propulsion systems of surrogate platforms. Sound levels at distances from the VSP airgun array and the drilling platform were predicted with a combination of underwater acoustic propagation models, in conjunction with the modelled source levels. These predictions account for sound sources directivity and the range-dependent environmental properties in the area.

The assessed sound level thresholds associated with injury and disturbance to marine mammals were based on peer-reviewed publications, including the 2016 National Oceanic and Atmospheric Administration (NOAA) Technical Guidance (NMFS 2016) for injury to marine mammals, and the current U.S. National Marine Fisheries Service (NMFS) criteria (NMFS 2013) for behavioural response by marine mammals.

Ambient levels derived from a data collection program conducted by JASCO in 2016–2017 are presented to summarize the soundscapes during the Project. The analysis of the data collected at Station 18 and 19 (Figure 1) focuses on the biological (marine mammal) and anthropogenic (seismic surveys, and oil and gas production activities) components of the soundscapes.

In this report, Section 2 discusses the methodology for modelling source levels and sound propagation, and for calculating ambient levels representative of the area. Section 3 describes the specifications of the sources, environmental parameters used in the propagation models, and the parameters used for calculating ambient levels. Section 3.4 presents the modelled results in two formats: tables of distances to sound levels thresholds associated to injury and disturbance criteria, and sound field contour maps showing the directivity and range to various sound level isopleths. This section also present ambient noise data as 1/3-octave-band levels over a full year, highlighting prominent biological and anthropogenic sounds. In Section 4.3.1, results are discussed relative to ambient noise levels in the area.

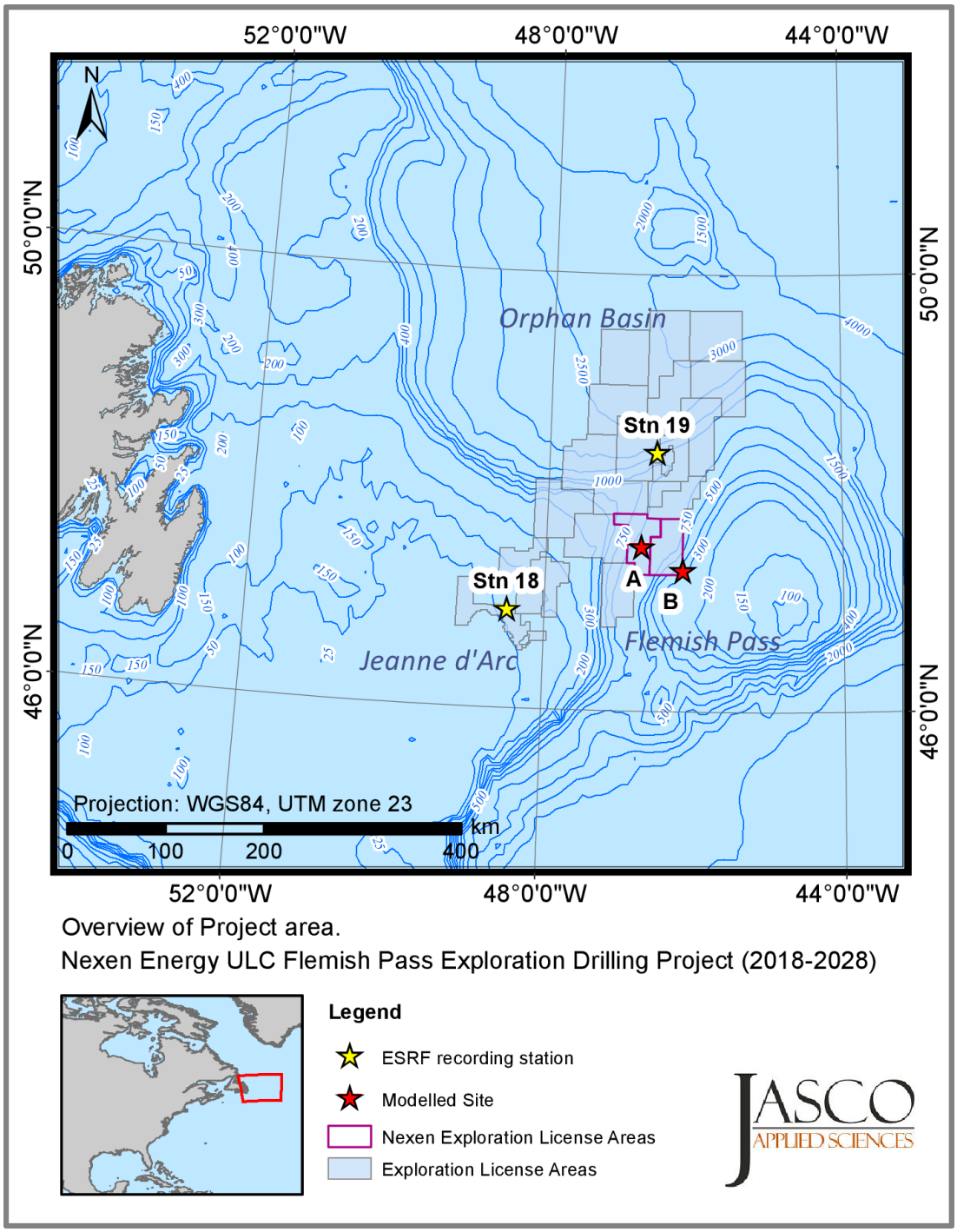

Overview of Project area.
Nexen Energy ULC Flemish Pass Exploration Drilling Project (2018-2028)

Figure 1. Overview of the project area, modelled sites, and ambient level recording stations.

1.1. Modelled Scenarios

Sound fields were modelled at two sites within the project area: Site A is a deep site in EL 1144, and Site B is a shallow site in EL 1150 (Figure 1; Table 1). At each site, the operation of a VSP airgun array and a drilling platform were modelled. At the time of this study, the VSP airgun array for the Project was yet not selected by Nexen. A 2400 in^3 array was selected as a surrogate for modelling based on previous work on the east coast of Canada (Zykov 2016). This array is expected to provide a conservative, yet realistic estimate of distances to impact criteria thresholds for typical VSP operations.

The drilling platform to be used in the Project was also not yet selected. A drillship and a semi-submersible platform were presented as possible drilling platforms. Based on previous work (Zykov 2016), it is expected that the semi-submersible platform will lead to longer distances to impact thresholds and, thus, was used in this study. The semi-submersible West Aquarius (from Seadrill) and the supply vessel the Avalon Sea (from the Secunda Canada fleet) were selected as surrogates for this study. Figure 2 shows the geometry of the drilling platform scenario, for which the actual location of each thruster was accounted for when the combined acoustic field around the platform was calculated.

Table 1. Modelled site locations and water depths.

Site	Latitude (N)	Longitude (W)	Water depth (m)
A	47° 31' 01.23"	46° 43' 09.20"	1137
B	47° 18' 13.21"	46° 09' 18.53"	378

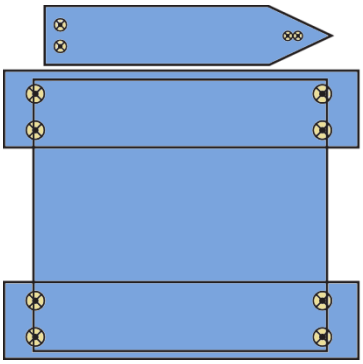

Figure 2. Geometry of semi-submersible platform with supply vessel. The circles indicate thruster locations.

1.2. Acoustic Impact Criteria

The perceived loudness of sound, especially impulsive noise such as from seismic airguns, is not generally proportional to the instantaneous acoustic pressure. Rather, perceived loudness depends on the time over which the pulse rises, its duration, and its frequency content. Thus, several sound level metrics are commonly used to evaluate noise and its effects on marine life. Table 2 lists the metrics applied in this report, peak pressure level (PK), root-mean-square (rms) sound pressure level (SPL), and sound exposure level (SEL) (see definitions in Appendix A.1). The acoustic metrics in this report reflect the updated ANSI and ISO standards for acoustic terminology, ANSI-ASA S1.1 (R2013) and ISO/DIS 18405.2:2017 (2016).

Whether acoustic exposure levels might injure or disturb marine mammals is an active research topic. Since 2007, several expert groups have investigated an SEL-based assessment approach for injury, with a handful of key papers published on the topic. The number of studies that investigate the level of

disturbance to marine animals by underwater noise has also increased substantially. Based on the best available science, the following sound level thresholds were assessed:

- M-weighted SEL and PK thresholds for injury to marine mammals, based on the 2016 NOAA Technical Guidance (NMFS 2016) (see Appendix A.3). SEL was assessed by integrating over 24 h.
- Behavioural thresholds due to impulsive sound sources based on the current NMFS criteria for marine mammals (NMFS 2013), i.e., 160 dB re 1 µPa (SPL) for the VSP airgun array and 120 dB re 1 µPa (SPL) for the semi-submersible with supply vessel.

The reported distances to all thresholds are calculated as maximum level over the entire water column. Details on each set of thresholds and the associated frequency-weighting are provided in Appendices A.2–A.3.

Table 2. NOAA 2016 marine mammal injury acoustic thresholds.

Hearing group	Impulsive source		Non-impulsive source
	PK	Weighted SEL (24 h)	Weighted SEL (24 h)
Low-frequency cetaceans	219	183	199
Mid-frequency cetaceans	230	185	198
High-frequency cetaceans	202	155	173
Phocid pinnipeds in water	218	185	201
Otariid pinnipeds in water	232	203	219

2. Method

2.1. Modelling Acoustic Sources

2.1.1. VSP Airgun Array

The source levels and directivity of the VSP airgun array were predicted with JASCO's Airgun Array Source Model (AASM), which accounts for:

- Array layout
- Volume, tow depth, and firing pressure of each airgun
- Interactions between different airguns in the array

The arrays' signatures were modelled over AASM's full frequency range, up to 25 kHz. Details of the model are described in Appendix A.5.1.

2.1.2. Drilling Platform

The source levels for each thruster on the semi-submersible platform and the supply vessel were modelled individually. The source level spectra were based on blade diameter and tip speed of a thruster, according to Ross (1976) and Brown (1977) equations and spectrum for sound generated by cavitation processes (Appendix A.5.2). When the blade diameter and tip speed of a thruster was unknown, we modelled the source level from a similar thruster, scaled according to the ratio of its maximum power.

2.2. Modelling Sound Propagation

Three sound propagation models (Appendix A.6) were used to predict the acoustic field around the airgun array for frequencies from 10 Hz to 25 kHz:

- Range-dependent parabolic equation model (Marine Operations Noise Model, MONM)
- Range-dependent ray tracing model (BELLHOP)
- Full Waveform Range-dependent Acoustic Model (FWRAM)

The models were used in combination to characterize the acoustic fields at short and long ranges in terms of SPL, PK, and SEL.

2.3. Estimating Ranges to Threshold Levels

Sound level contours were calculated based on the underwater sound fields predicted by the propagation models, sampled by taking the maximum value over all modelled depths above the seafloor for each location in the modelled region. The predicted distances to specific levels were computed from these contours. Two distances relative to the source are reported for each sound level: 1) R_{max}, the maximum range to the given sound level over all azimuths, and 2) $R_{95\%}$, the range to the given sound level after the 5% farthest points were excluded (see examples in Figure 3).

The $R_{95\%}$ is used because sound field footprints are often irregular in shape. In some cases, a sound level contour might have small protrusions or anomalous isolated fringes. This is demonstrated in the image in Figure 3(a). In cases such as this, where relatively few points are excluded in any given direction, R_{max} can misrepresent the area of the region exposed to such effects, and $R_{95\%}$ is considered more

representative. In strongly asymmetric cases such as shown in Figure 3(b), on the other hand, $R_{95\%}$ neglects to account for significant protrusions in the footprint. In such cases R_{max} might better represent the region of effect in specific directions. Cases such as this are usually associated with bathymetric features affecting propagation. The difference between R_{max} and $R_{95\%}$ depends on the source directivity and the non-uniformity of the acoustic environment.

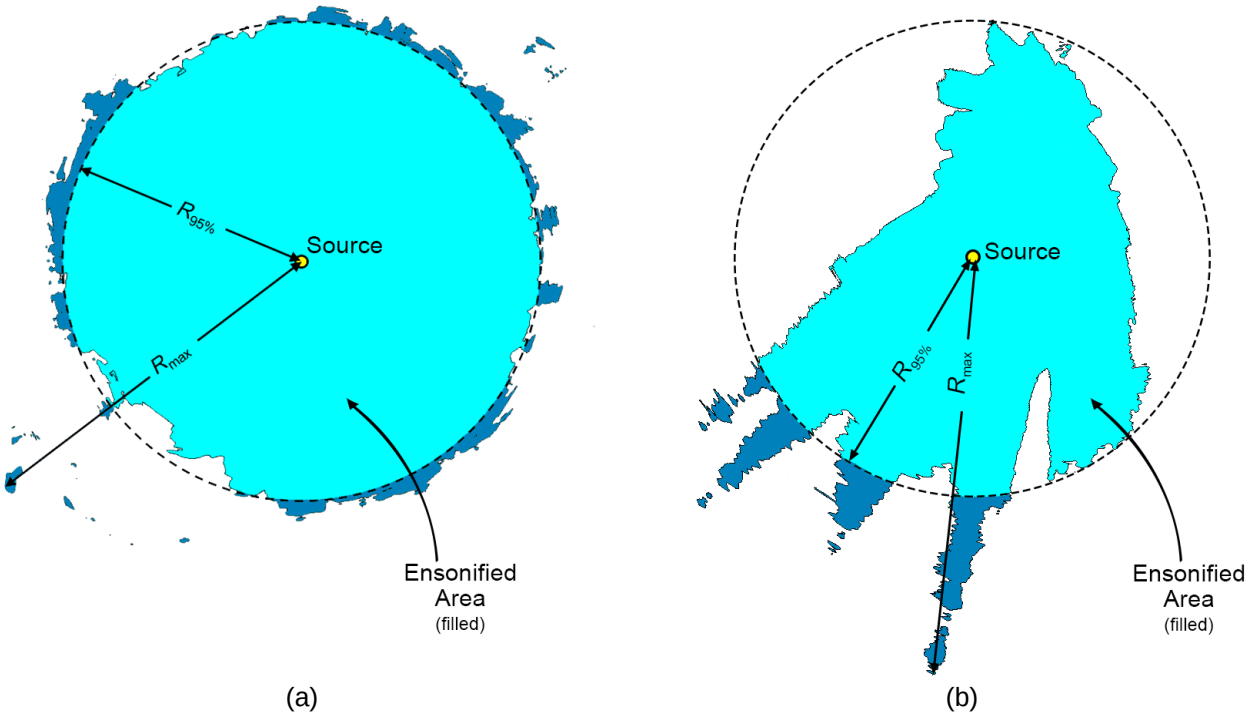

Figure 3. Sample areas ensonified to an arbitrary sound level with R_{max} and $R_{95\%}$ ranges shown for two different scenarios. (a) Largely symmetric sound level contour with small protrusions. (b) Strongly asymmetric sound level contour with long protrusions. Light blue indicates the ensonified areas bounded by $R_{95\%}$; darker blue indicates the areas outside this boundary which determine R_{max}.

2.4. Estimating SPL from Modelled SEL Results

The per-pulse SEL of sound pulses is an energy-like metric related to the dose of sound received over a pulse's entire duration. The pulse SPL on the other hand, is related to its intensity over a specified time interval. Seismic pulses typically lengthen in duration as they propagate away from their source, due to seafloor and surface reflections, and other waveguide dispersion effects. The changes in pulse length, and therefore the time window considered, affect the numeric relationship between SPL and SEL. This study has applied a fixed window duration to calculate SPL (T_{fix} = 125 ms) (Appendix A.1), as implemented in Martin et al. (2017). Full-waveform modelling was used to estimate SPL, but this type of modelling is computationally intensive, and can be prohibitively time consuming when run at high spatial resolution over large areas.

The SEL of a single-pulse is related to the SPL only by the pulse length; therefore, the SPL over a wide area can be calculated from the single-pulse SEL generated by MONM and BELLHOP. For the current study, Full Waveform Range-dependent Acoustic Model (FWRAM; Appendix A.6.3) is used to model synthetic pulses along 4 radials at each modelling site, up to a distance of 30 km. The synthetic pulses are analyzed to determine pulse length versus depth, distance, and azimuth from the source. The pulse lengths are averaged in 2 km bins along the radials, and extrapolated as constant at distances greater than 30 km. The results are used to derive a conversion function between single-pulse SEL and SPL (Figure 4). The range-dependent conversion function is applied to predicted per-pulse SEL results from MONM and BELLHOP to model SPL values in a 360° field.

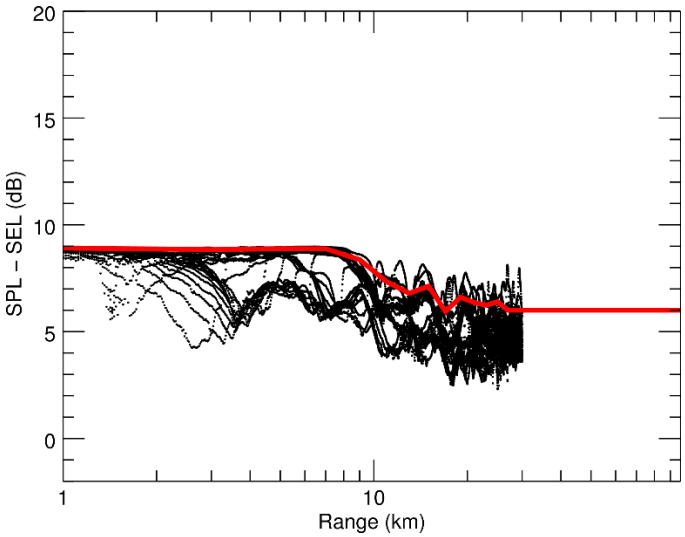

Figure 4. Range-dependent conversion function for converting per-pulse SEL to SPL for the 2400 in^3 airgun array pulses at Site A.

2.5. Estimating SEL over a 24 h period

During a VSP survey, new sound energy is introduced into the environment with each pulse from the airgun array. While some impact criteria are based on per-pulse energy released, others, such as the SEL criteria used in this report (Section 1.2), consider the total acoustic energy marine fauna is subjected to over 24 hours. An accurate assessment of the cumulative acoustic field depends not only on the parameters of each impulse, but also on the number of impulses delivered over the accumulation period and the relative position of the impulses. For this study, the VSP airgun array was assumed stationary, delivering 2000 pulses over the accumulation period (24 h).

The same principle applies to non-impulsive sources: SEL criteria consider the total acoustic energy marine fauna is subjected to over 24 hours. Here, the assessment of the cumulative acoustic field depends on the number of seconds of operation over the accumulation period. The semi-submersible and the supply vessels were assumed stationary, and to be operating continuously over the entire 24 h.

These assumptions provide a conservative assessment of the distances to impact thresholds.

2.6. Ambient Levels

The Canadian Atlantic seaboard is home to a wealth of marine life and the site of diverse human activities, including oil and gas activities, fishing, and shipping. To varying degrees, these anthropogenic activities all contribute to the soundscape of the surrounding waters. To summarize the soundscapes during the Project , we present the distribution of one-minute SPL from a data collection program conducted by JASCO in 2016–2017 (Section 3.4). We present an analysis of these JASCO recordings, focusing on the biological (marine mammal) and anthropogenic (seismic surveys, and oil and gas production activities) component of the soundscapes. The ambient, or background, sound levels that create the ocean soundscape are comprised of many natural and anthropogenic sources (Figure 5). Table 3 provides a classification of known biologic, man-made, natural and geologic, and measurement-noise mechanisms, as well as the frequency bands associated with their contributions to the soundscape. The main environmental (natural and geologic) sources of sound are wind, precipitation, and sea ice. Wind-generated noise in the ocean is well-described (e.g., Wenz 1962, Ross 1976), and surf noise is known to be an important contributor to near-shore soundscapes (Deane 2000). Precipitation is a frequent noise source, with contributions typically concentrated at frequencies above 500 Hz. At low frequencies (<100 Hz), earthquakes and other geological events contribute to the soundscape.

Anthropogenic sources in the region are primarily at low frequencies (<225 Hz) and include seismic activity and shipping noise.

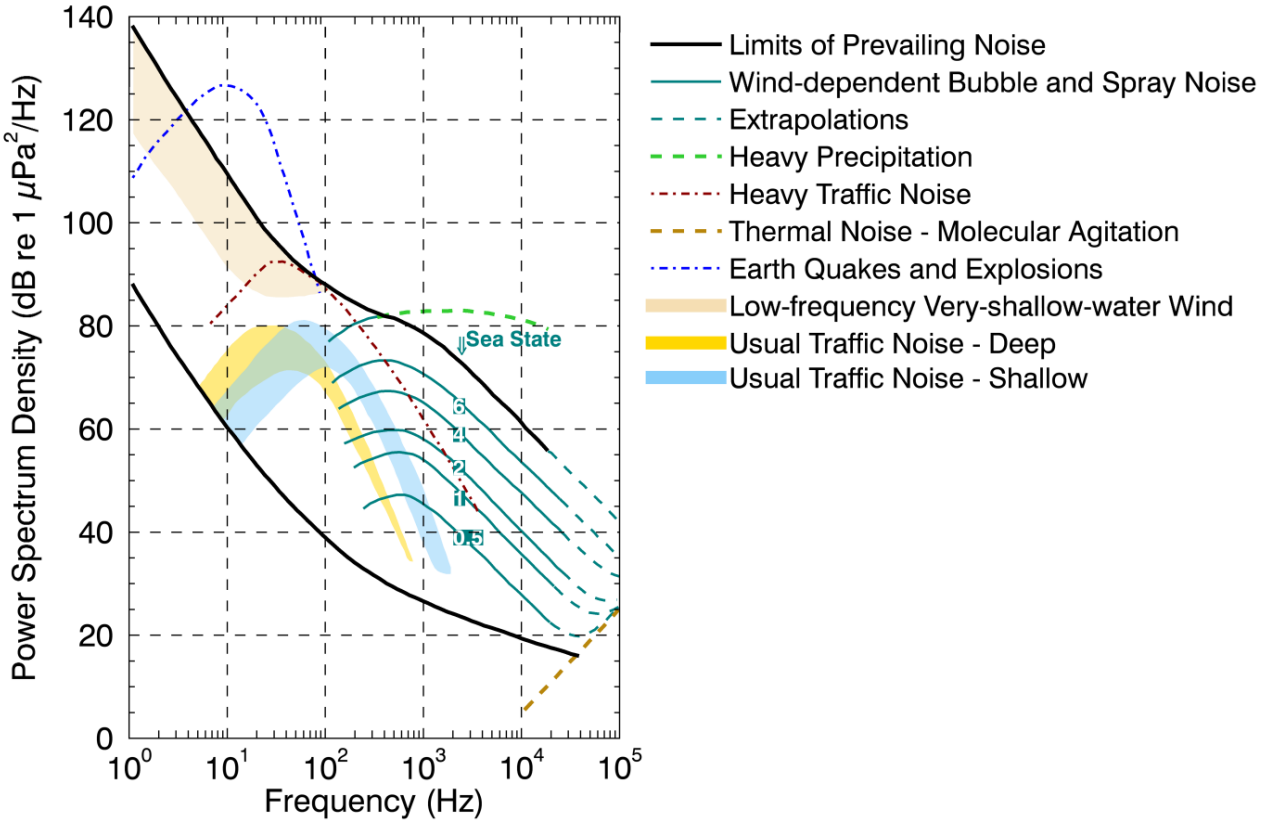

Figure 5. Wenz curves (NRC 2003), describing pressure spectral density levels of marine ambient noise from weather, wind, geologic activity, and commercial shipping, adapted from Wenz (1962).

Table 3. Typical sound generating mechanisms and their associated frequency bands.

Band name and frequency range	Sound source type			
	Biologic	Man-made	Natural and geologic	Measurement system noise
Very low frequency: 10–45 Hz	Fin and blue whales	Seismic pulses	Earthquakes	Flow noise, strum
Low frequency: 45–225 Hz	Fish, baleen whales, pinnipeds	Seismic pulses, large vessels	-	Flow noise, strum
Mid frequency: 225–2250 Hz	Baleen whales, fish, pinnipeds	Smaller vessels, large vessels at close range, DP	Wind and wave action	-
High frequency: 2250–18000 Hz	Whistles, sperm whale clicks, baleen songs, shrimp	Naval sonar, cavitation bubbles, chains	Sediment movement, rain	-
Very high frequency: >18000 Hz	Echolocation clicks	Communicating and positioning devices, naval sonar	-	-

"-" symbol means that the corresponding sound source does not have significant energy within the band.

3. Model Parameters

3.1. Acoustic Source Parameters

3.1.1. VSP Airgun Array

The Schlumberger Dual Magnum 2400 in^3 airgun, previously used by BP for a similar survey (Zykov 2016), was modelled as a surrogate seismic source for the VSP source. The Schlumberger airgun array consists of four triangular clusters with in-line separations of 2 m. Two clusters are assembled from three 250 in^3 source elements with 0.9 m separation between each element. The two other clusters have three 150 in^3 source elements with 0.6 m separation between each element. The airguns are activated simultaneously at 2000 psi air pressure. The airgun array was modelled at a tow depth of 4.5 m (the centre of the clusters). Figure 6 presents the airgun distribution in the horizontal (*x*-*y*) plane. Table 4 lists the layout of the VSP airgun array.

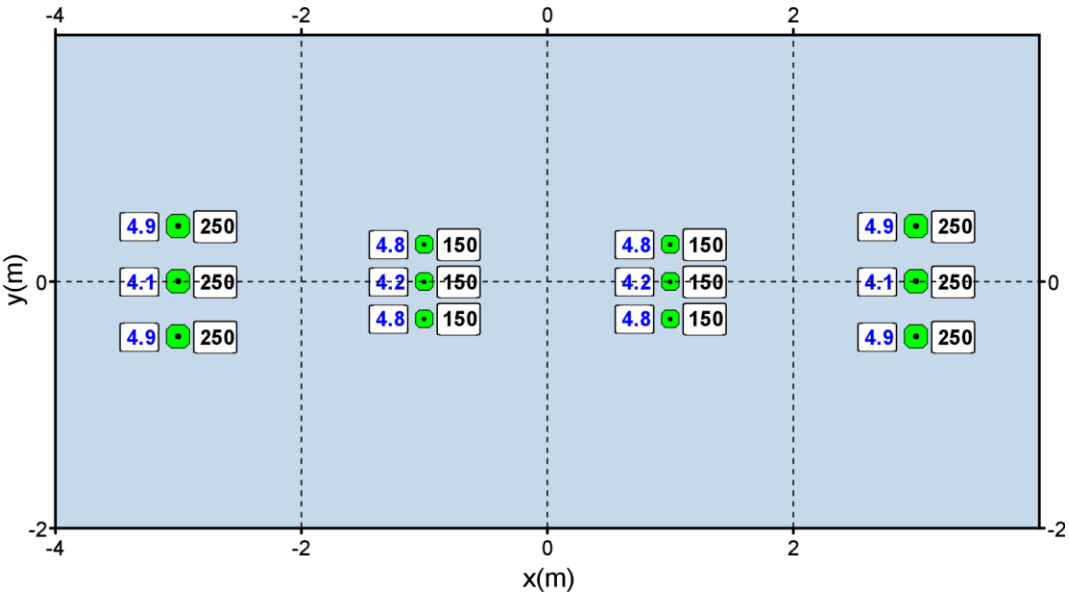

Figure 6. Layout of the 2400 in^3 airgun array, composed of 12 airguns. Relative symbol sizes and black numbers indicate airgun firing volume in cubic inches. The blue numbers indicate the depth of the source element relative to the sea surface.

Table 4. Layout of the 2400 in^3 airgun array. The firing pressure for all guns is 2000 psi.

Gun	*x* (m)	*y* (m)	*z* (m)	Volume (in^3)	Gun	*x* (m)	*y* (m)	*z* (m)	Volume (in^3)
1	−3	1	4.9	250	7	1	0.75	4.8	150
2	−3	0	5.1	250	8	1	0	4.2	150
3	−3	−1	4.9	250	9	1	0.75	4.8	150
4	−1	0.75	4.8	150	10	3	1	4.9	250
5	−1	0	4.2	150	11	3	0	4.1	250
6	−1	−0.75	4.8	150	12	3	1	4.9	250

3.1.2. Drilling Platform

The surrogate drilling platform used in this study is a semi-submersible platform equipped with dynamic positioning system. The primary noise source for the vessel is the thrusters. The surrogate semi-submersible platform is the West Aquarius (Figure 7), which is equipped with eight UUC 355 thrusters, located at the corners of the platform in pairs. The estimated source levels from individual thrusters are based on the nominal top rotation speed (revolution per minute (rpm)). The depth of the sound source (i.e., the depth of the thrusters) was set to 23 m, the maximum depth of the platform. Although the speed and vertical position of the thrusters will vary based on the environmental conditions and the platform load, it is expected that the difference would not substantially impact on the size of acoustic footprint. All parameters were chosen to produce a conservative estimate of the distances to impact thresholds. Table 5 presents the characteristics of the thrusters.

Figure 7. West Aquarius. Photo from Seadrill (http://www.seadrill.com/our-fleet.aspx).

The surrogate supply vessel modelled alongside the semi-submersible is the Avalon Sea (Figure 8). This vessel is expected to use dynamic positioning to maintain station alongside the semi-submersible. In dynamic positioning mode, two bow thrusters and two stern thrusters are used (Table 5). Since little information on the type, size, and speed of these thrusters is available, source levels for similar thrusters (Zykov 2016) were scaled according to the difference in maximum power. Similarly to the semi-submersible, variation in environmental condition and load could change the thrusters' vertical position and rpm. However, the estimated source levels are considered conservative since levels are scaled to the maximum power.

Figure 8. Avalon Sea. Photo from MarineTraffic (http://www.marinetraffic.com/en/ais/details/ships/shipid:4006445/mmsi:316001380/vessel:AVALON SEA).

Table 5. Characteristics of the semi-submersible and supply vessel.

Sound source		Propeller diameter (m)	Nominal propeller speed (rpm)	Max. power (kW)	Number of thrusters	Thruster model	Number of blades	Acoustic source depth (m)
Semi-submersible (West Aquarius)	All thrusters	3.5	177	3800	8	UUC355	4	23
Supply vessel (Avalon Sea)	Azimuth (bow) thruster	Unknown	Unknown	1200	1	Unknown (azimuthal)	Unknown	5
	Bow thruster	Unknown	Unknown	1150	1	Unknown (tunnel)	Unknown	5
	Stern thrusters	Unknown	Unknown	1050	2	Unknown (tunnel)	Unknown	5

3.2. Environmental Parameters

3.2.1. Bathymetry

Water depths throughout the modelled area (>100 km around Site A and Site B) were extracted from the SRTM15+ global bathymetry grid, a 15 arc-second grid (~300 × 500 m at the studied latitude) rendered for the entire globe (Rodríguez et al. 2005). The water depth in the Flemish Pass area varies from 200–300 m in the southwest section (toward the Jeanne D'Arc Basin) to >3000 m northeast of the Flemish Cap (Figure 1). The water depths in the Jeanne D'Arc Basin area range from <80 m on the Grand Banks to more than 2000 m southeast of the Flemish Cap.

3.2.2. Geoacoustic Profiles

The geoacoustic properties of surficial layers depend on the sediment type. As the porosity decreases, the compressional sound speed, sediment bulk density, and compressional attenuation increase. For both modelled sites, MONM assumes a single geoacoustic profile of the seafloor for the entire modelled area. The acoustic properties required by MONM are:

- Sediment bulk density,
- Compressional-wave (or P-wave) speed, P-wave attenuation in decibels per wavelength,
- Shear-wave (or S-wave) speed, and
- S-wave attenuation, also in decibels per wavelength.

These geoacoustic parameters for the sediment layer were estimated using a sediment grain-shearing model (Buckingham 2005), which computes the acoustic properties of the sediments from porosity and grain-size measurements. The input parameters required by the geoacoustic model are the bottom type (grain size) and sediment porosity, inferred from the geological description of the modelling region. The geoacoustic profile (Table 6) was based on data obtained by the Ocean Drilling Program (ODP) at site 905, leg 150 (Shipboard Scientific Party 1994). The ODP well was located at a 2,700 m water depth. The reported porosity for the surficial sediments is 60% and does not change with depth, maintaining the same value of 60% down to 600 metres below the seafloor (mbsf).

On the Grand Banks continental shelf, through the Flemish Pass, and in the southern Orphan Basin, the shallow sedimentary layers consist of thick grey muds (silt mixed with 10–30% sand and 20–40% clay) with varying amounts of debris and sand bed horizons (Huppertz 2007). The shallow depths (~1100 m) and narrow banks of the Flemish Pass trap sediment deposits from the continental shelf.

Two generic geoacoustic profiles were constructed for the region, based on water depth. A thick layer of silt/mud was assumed for both profiles. The average grain size of the silt was assumed to decrease with increasing water depth. Representative grain sizes and porosity were used in the grain-shearing model proposed by Buckingham (2005) to estimate the geoacoustic parameters that would be required by sound propagation models. Tables 6 and 7 list the geoacoustic parameters derived for numeric modelling.

Table 6. *Deep water (Site A, 1137 m)*: Geoacoustic parameters derived for Eastern Newfoundland Exploration Drilling Project Area.

Depth below seafloor (m)	Material	Density (g/cm³)	P-wave speed (m/s)	P-wave attenuation (dB/λ)	S-wave speed (m/s)	S-wave attenuation (dB/λ)
0–5	Silt mixed with sand and clay	1.5–1.7	1525–1585	0.25–0.40	130	3.65
5–50		1.7–2.0	1585–1775	0.40–0.75		
50–500		2.0–2.1	1775–2100	0.75–1.40		
>500		2.1	2100	1.40		

Table 7. *Shallow water (Site B, 387 m)*: Geoacoustic parameters derived for Eastern Newfoundland Exploration Drilling Project Area.

Depth below seafloor (m)	Material	Density (g/cm³)	P-wave speed (m/s)	P-wave attenuation (dB/λ)	S-wave speed (m/s)	S-wave attenuation (dB/λ)
0–5	Silt mixed with sand and clay	1.5–1.7	1560–1650	0.40–0.65	200	3.65
5–50		1.7–2.0	1650–1910	0.65–1.15		
50–500		2.0–2.1	1910–2435	1.15–2.00		
>500		2.1	2435	2.00		

3.2.3. Sound Speed Profiles

The sound speed profiles for the modelled sites were derived from temperature and salinity profiles from the U.S. Naval Oceanographic Office's *Generalized Digital Environmental Model V 3.0* (GDEM; Teague et al. 1990, Carnes 2009). GDEM provides an ocean climatology of temperature and salinity for the world's oceans on a latitude-longitude grid with 0.25° resolution, with a temporal resolution of one month, based on global historical observations from the U.S. Navy's Master Oceanographic Observational Data Set (MOODS). The climatology profiles include 78 fixed depth points to a maximum depth of 6800 m (where the ocean is that deep). The GDEM temperature-salinity profiles were converted to sound speed profiles according to Coppens (1981).

Mean monthly sound speed profiles were derived from the GDEM profiles for the probable operational months (January to December; Figure 9). Profiles for January to May are least least downward refracting. Sound is therefore expected to propagated to longer distances during this period. From December to April, VSP operations would be difficult because of the heavy weather and sea state conditions in the area. There are usually fewer antropogenic activities during these months. May was selected for modelling since this profile is the least downward refracting during the months that are traditionally most operationally active (May to October). Thus, using the sound speed profile for May will result in conservative but realistic distances to the assessed sound thresholds compared to the yearly averaged.

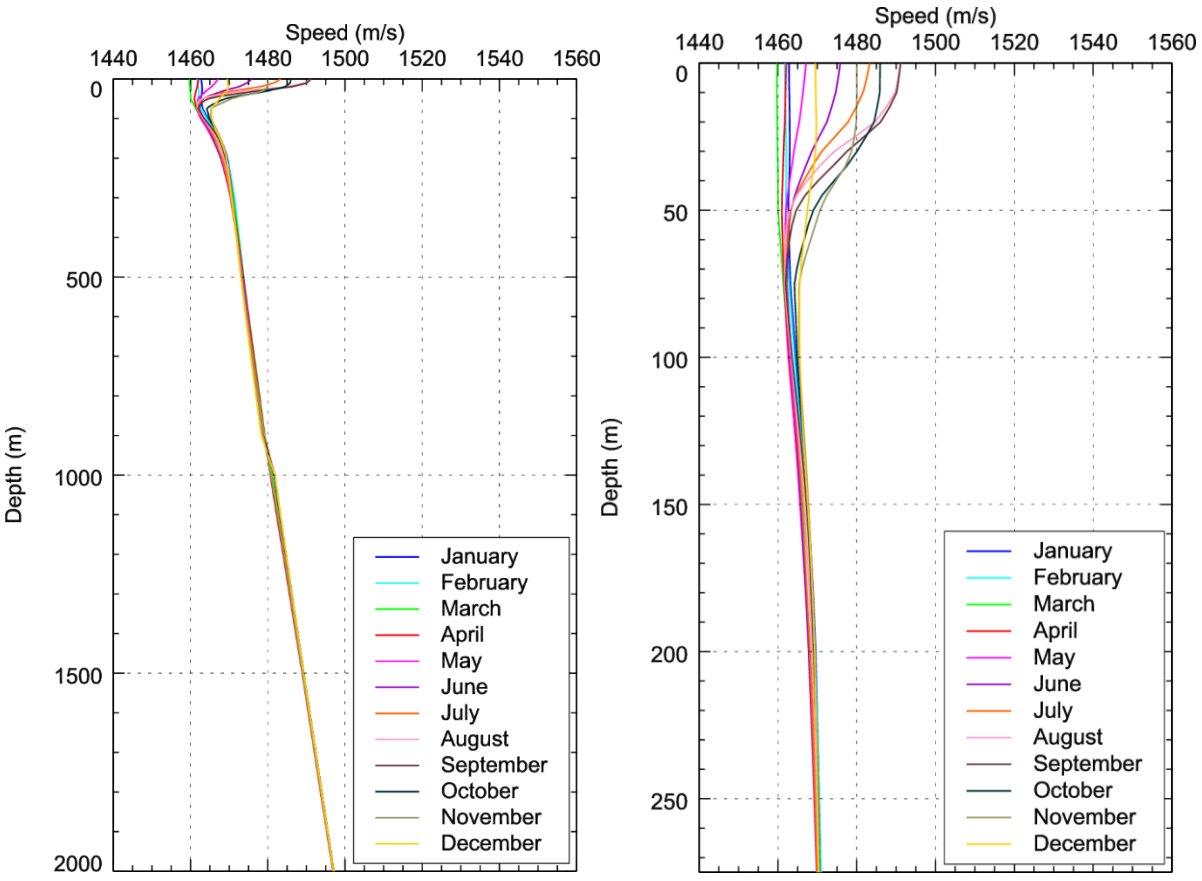

Figure 9. Mean monthly sound speed profiles at Site A for the full water column (left) and top 275 m depth (right), derived from data obtained from *GDEM V 3.0* (Teague et al. 1990, Carnes 2009). Profiles at Site B are similar.

3.3. Sound Propagation

The per-pulse SEL sound field from a single VSP airgun array pulse was modelled for 1/3-octave-bands from 10 Hz to 25 kHz using MONM (10 Hz to 1 kHz) and BELLHOP (1.25 to 25 kHz). Each frequency band was modelled from the source along 72 radial planes (horizontal angular resolution $\Delta\theta = 5°$) with a 20 m horizontal step size, up to a maximum distance of 100 km. To obtain the vertical distribution of the acoustic field, at each surface grid point the sound field was sampled at 28 depths from 2 to 2000 m, with increasing depth steps (from 5 to 250 m). The per-pulse SEL were then summed across frequencies and gridded to a cartesian coordinate system with a regular grid spacing of 20 m. SPL sounds fields were calculated from the SEL fields using a range-dependent broadband conversion factor (Section 2.4).

PK for the VSP airgun array were modelled using FWRAM at frequencies of 10–2048 Hz, along 4 radials with a 20 m horizontal step size, to a maximum distance of 30 km.

3.4. Ambient Levels

In July 2016, JASCO deployed 20 acoustic recorders along Canada's east coast for the second year of a two-year baseline monitoring program sponsored by the Environmental Sciences Research Fund (ESRF). The recorders were retrieved in July 2017. Data from two of these recorders are discussed here, as they provide the best available information on the existing sound levels in the Project Area (Figure 1).
ESRF Station 18 was in shallow water at a depth of 214 m, 140 km east of Site A and 28 km from the Hibernia platform in the existing Jeanne D'Arc Basin development area. ESRF Station 19 was in deep water (>1500 m) in the Flemish Pass, ~100 km north of Site A. The locations of both stations are provided in Table 8.

Table 8. JASCO recorder locations.

ESRF station	Latitude	Longitude	Depth
18	46° 54.708	048° 30.069	214
19	48° 22.812	046° 31.526	1547

4. Results

4.1. Source Levels and Directivity

4.1.1. VSP Airgun Array

The horizontal overpressure signatures and corresponding power spectrum levels for the 2400 in^3 array were computed at frequencies up to 25 kHz. They are shown in Figure 10 for the broadside (perpendicular to the tow direction), and endfire (parallel to the tow direction), up to 2.5 kHz. The signatures consist of a strong primary peak related to the initial firing of the airgun, followed by a series of pulses associated with bubble oscillations. Most energy is produced at frequencies below 500 Hz. The spectrum contains peaks and nulls resulting from interference among airguns in the array, where the frequencies at which they occur depend on the volumes of the airguns and their locations within the array.

Horizontal PK and SEL also show the source level difference between the broadside and endfire directions. For this array, PK and SEL in the broadside direction were estimated to be 248.2 dB re 1 µPa and 224.7 dB re 1 µPa^2·s, respectively, and in the endfire direction they were estimated to be slightly lower at 245.6 dB re 1 µPa and 224.1dB re 1 µPa^2·s, respectively (Table 9).

Figure 11 shows the horizontal 1/3-octave-band directivities for the array. In these plots, the arrow indicates the tow direction of the array and the solid black curves indicate source levels in dB re 1 µPa^2·s, as a function of angle in the horizontal plane, referenced to a fixed radial decibel level scale (dashed circles).

The general trend for the spectral levels is to decrease with increasing frequency. The source directivity becomes significant above 150 Hz, while most of the array energy is contained in frequencies up to 500 Hz, implying that a significant amount of energy does not equally propagate in all directions.

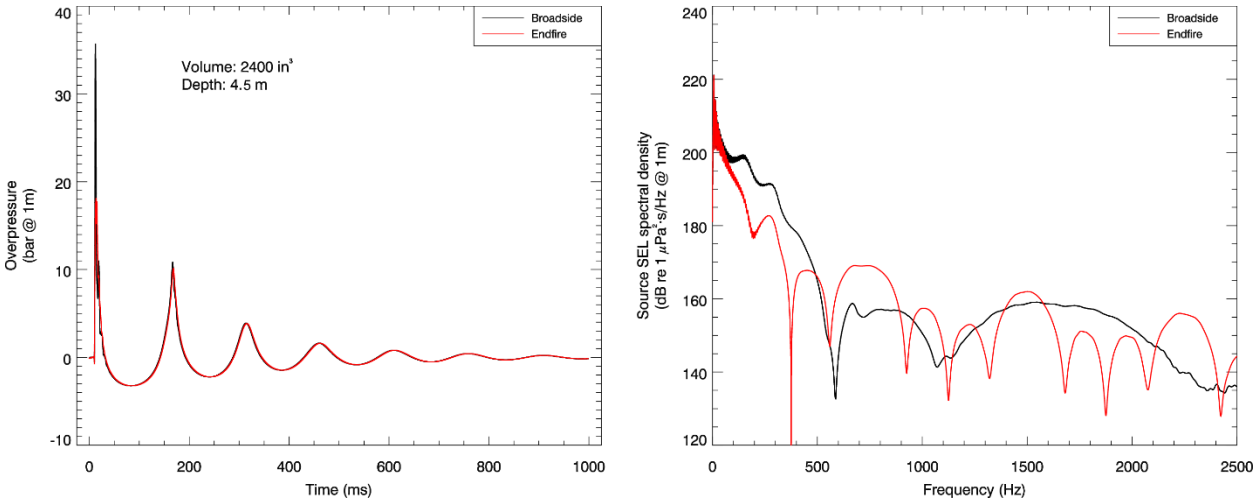

(a) (b)

Figure 10. Predicted a) overpressure signature and b) power spectrum in the broadside and endfire (horizontal) directions for the 2400 in^3 array. Surface ghosts (effects of the pulse reflection at the water surface) are not included in these signatures as they are accounted for by the propagation models.

Table 9. Horizontal source level specifications (0.01–25 kHz) for the 2400 in^3 airgun array at a 4.5 m tow depth, computed with Airgun Array Source Model (AASM) in the broadside and endfire directions.

Direction	Zero-to-peak SPL (dB re 1 µPa @ 1 m)	SEL (dB re 1 µPa^2·s @ 1 m)			
		0.01–25 kHz	0.01–0.5 kHz	0.5–5 kHz	5–25 kHz
Broadside	248.2	224.7	224.7	192.5	171.6
Endfire	245.6	224.1	224.1	195.0	172.2

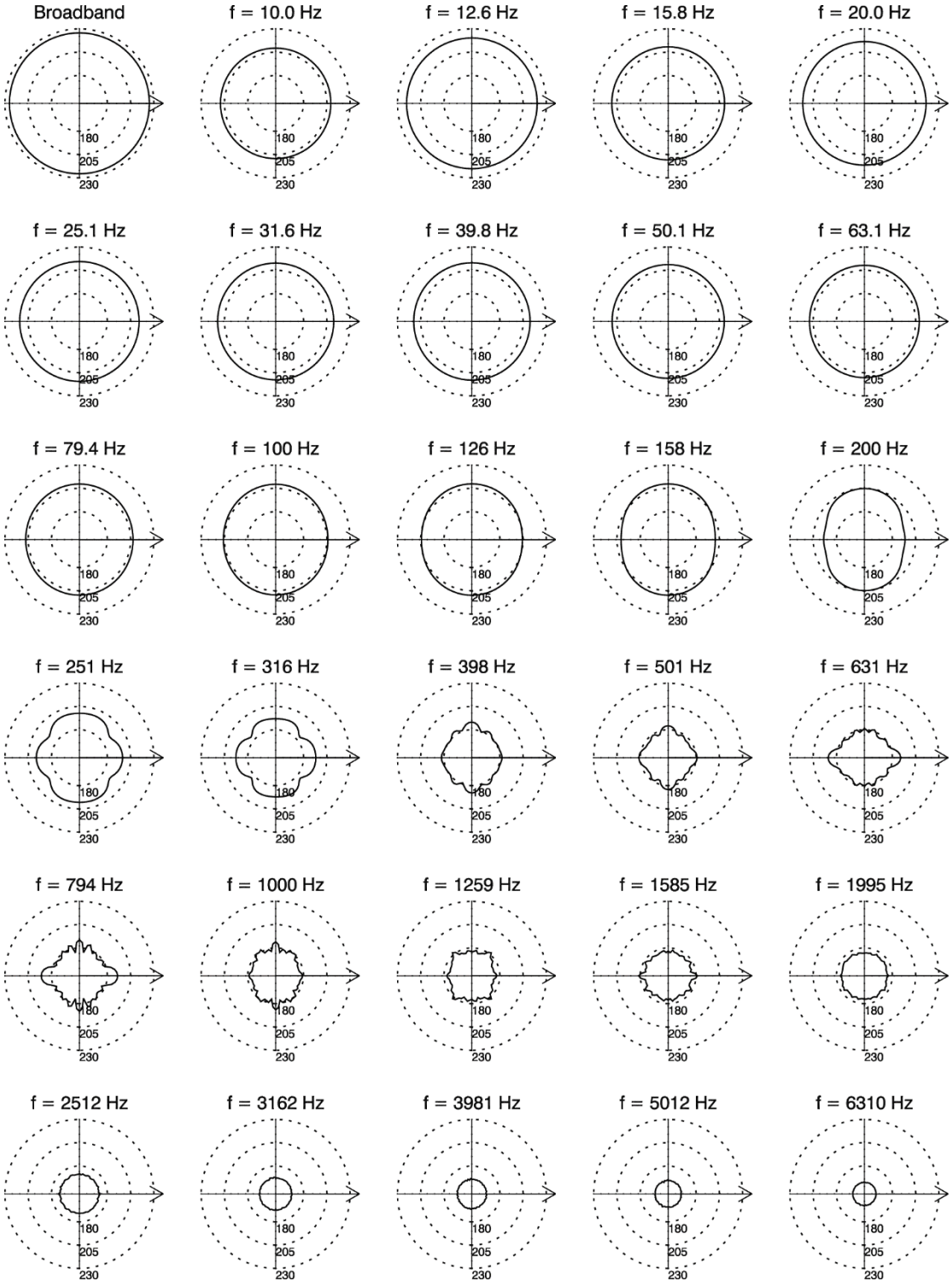

Figure 11. Directionality of predicted horizontal source levels (SL, dB re 1 $\mu Pa^2 \cdot s$) in 1/3-octave-bands for the modelled 2400 in^3 airgun array, at 4.5 m tow depth. The 1/3-octave-band centre frequencies are indicated above each plot.

4.1.2. Drilling Platform

The source levels and the sound spectrum from thrusters on the surrogate semi-submersible and supply vessel were estimated based on the thruster specifications (diameter, rpm, or maximum power), according to the method described in Section 3.1.2 and Appendix A.5.2. The method assumes that under heavy operation conditions, the sound from cavitation dominates over sound from other components (machinery, drilling equipment, hull vibration). The relative spectrum of the sound is identical for all thrusters, as the method only accounts for the change of the broadband source level. The thrusters are considered as omni-directional sources (i.e., the source levels do not depend on the horizontal azimuth). Directionality on the sound field around the drilling platform is due to the relative position of each thruster. Table 10 provides the estimated broadband levels of the individual modelled thrusters, and Figure 12 shows their sound spectra.

Table 10. Estimated broadband levels for individual thrusters.

Sound source		Broadband source level (dB re 1 µPa @ 1 m)
Semi-submersible (West Aquarius)	All thrusters	187.71
Supply vessel (Avalon Sea)	Azimuth (bow) thruster	180.65
	Bow thruster	180.63
	Stern thrusters	180.60

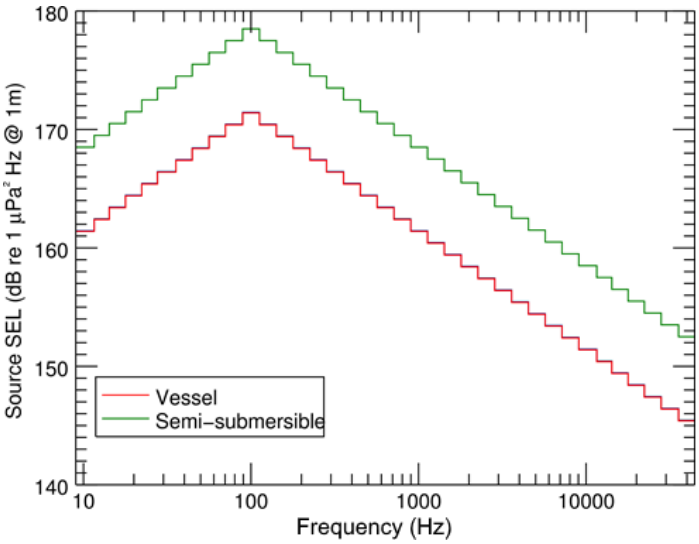

Figure 12. Estimated sound spectra from cavitating propellers of individual thrusters.

4.2. Acoustic Fields

This section presents modelled sound fields as root-mean-square (rms) sound pressure levels (SPL), peak pressure levels (PK), and sound exposure levels (SEL_{24h}) in two formats: as tables of distances to sound levels and, where the distances are long enough, and as contour maps showing the directivity and range to various sound levels.

Distances to thresholds are reported as R_{max} and $R_{95\%}$ (Section 2.3). The underwater sound field predicted by the propagation models was sampled such that the received sound level at each point in the horizontal plane was taken to be the maximum value over all modelled depths for that point. Tables 11 and 12 summarize the distances marine mammal thresholds at the two modelling sites.

Table 11. *Site A*: Distances (km) to behavioural and injury thresholds based on NMFS (2013) and (2016). SEL_{24h} results were calculated from M-weighted sound fields using the appropriate frequency filter for each hearing group.

Hearing group	Behavioural			Injury					
	SPL threshold (dB re 1 µPa)	R_{max}	$R_{95\%}$	PK threshold (dB re 1 µPa)	R_{max}	$R_{95\%}$	SEL_{24h} threshold (dB re 1 µPa²·s)	R_{max}	$R_{95\%}$
VSP airgun array									
Low-frequency cetaceans	160	6.35	5.26	219	<0.02	<0.02	183	4.98	4.58
Mid-frequency cetaceans	160	6.35	5.26	230	<0.02	<0.02	185	-	-
High-frequency cetaceans	160	6.35	5.26	202	0.12	0.12	155	0.16	0.14
Phocid pinnipeds in water	160	6.35	5.26	218	<0.02	<0.02	185	0.38	0.34
Otariid pinnipeds in water	160	6.35	5.26	232	<0.02	<0.02	203	0.02	0.02
Drilling platform									
Low-frequency cetaceans	120	47.61	38.07	n/a	n/a	n/a	199	0.23	0.22
Mid-frequency cetaceans	120	47.61	38.07	n/a	n/a	n/a	198	0.18	0.16
High-frequency cetaceans	120	47.61	38.07	n/a	n/a	n/a	173	1.88	1.72
Phocid pinnipeds in water	120	47.61	38.07	n/a	n/a	n/a	201	0.16	0.15
Otariid pinnipeds in water	120	47.61	38.07	n/a	n/a	n/a	219	0.15	0.14

"-" symbol means the level was not reached.

Table 12. *Site B*: Distances (km) to behavioural and injury thresholds based on NMFS (2013) and (2016). SEL_{24h} results were calculated from M-weighted sound fields using the appropriate frequency filter for each hearing group.

Hearing group	Behavioural			Injury					
	SPL threshold (dB re 1 µPa)	R_{max}	$R_{95\%}$	PK threshold (dB re 1 µPa)	R_{max}	$R_{95\%}$	SEL_{24h} threshold (dB re 1 µPa²·s)	R_{max}	$R_{95\%}$
VSP airgun array									
Low-frequency cetaceans	160	7.86	6.10	219	<0.02	<0.02	183	9.66	5.98
Mid-frequency cetaceans	160	7.86	6.10	230	<0.02	<0.02	185	-	-
High-frequency cetaceans	160	7.86	6.10	202	120	120	155	0.16	0.14
Phocid pinnipeds in water	160	7.86	6.10	218	<0.02	<0.02	185	0.38	0.34
Otariid pinnipeds in water	160	7.86	6.10	232	<0.02	<0.02	203	0.02	0.02
Drilling platform									
Low-frequency cetaceans	120	56.78	40.58	n/a	n/a	n/a	199	0.23	0.22
Mid-frequency cetaceans	120	56.78	40.58	n/a	n/a	n/a	198	0.18	0.16
High-frequency cetaceans	120	56.78	40.58	n/a	n/a	n/a	173	3.29	3.04
Phocid pinnipeds in water	120	56.78	40.58	n/a	n/a	n/a	201	0.16	0.15
Otariid pinnipeds in water	120	56.78	40.58	n/a	n/a	n/a	219	0.15	0.14

"-" symbol means the level was not reached.

4.2.1. Sound Pressure Levels (SPL)

Table 13 presents the distances to the sound levels thresholds from 200 to 120 dB re 1 µPa (SPL) in 10 dB steps and to NMFS criteria thresholds (values in bold) for the VSP airgun array and the drilling platform, at the two modelling sites. Figures 13–16 present the associated sound fields as maximum-over-depth contour maps, showing the directivity and range to sound levels in 10 dB steps.

Table 13. Maximum (R_{max}) and 95% ($R_{95\%}$) horizontal distances (km) from the VSP airgun array and the centre of the drilling platform to modelled maximum-over-depth root-mean-square sound pressure level thresholds (SPL; dB re 1 µPa). Values in bold indicate NMFS criteria thresholds for marine mammals (160 dB re 1 µPa for impulsive sources and 120 dB re 1 µPa for non-impulsive sources).

SPL (dB re 1 µPa)	**VPS airgun array**				**Drilling platform**			
	Site A		Site B		Site A		Site B	
	R_{max}	$R_{95\%}$	R_{max}	$R_{95\%}$	R_{max}	$R_{95\%}$	R_{max}	$R_{95\%}$
200	0.04	0.040	0.040	0.040	-	-	-	-
190	0.14	0.126	0.141	0.140	-	-	-	-
180	0.44	0.400	0.444	0.405	-	-	0.10	0.09
170	1.41	1.266	1.970	1.738	0.10	0.09	0.15	0.14
160	**6.35**	**5.264**	**7.860**	**6.103**	0.16	0.149	0.16	0.15
150	20.69	18.136	21.291	17.139	0.34	0.324	0.34	0.33
140	57.76	43.426	100.000	91.216	1.07	1.041	1.77	1.69
130	>100.0	-	>100.0	-	5.62	5.374	12.16	9.42
120	-	-	-	-	**47.61**	**38.07**	**56.78**	**40.58**

"-" symbol means the level was not reached.

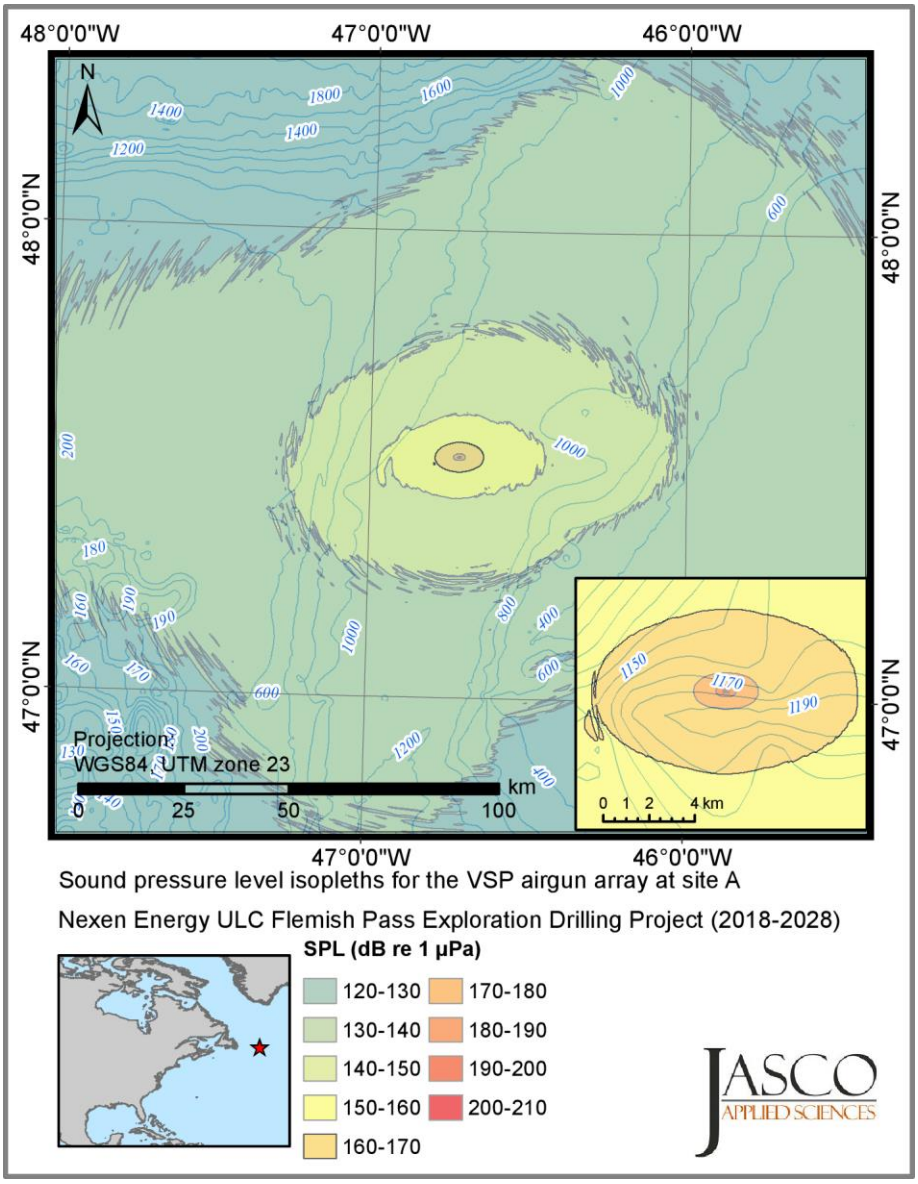

Figure 13.*Site A, VSP airgun array*: Broadband (10–25,000 Hz) maximum-over-depth SPL field. Blue contours indicate water depth in metres.

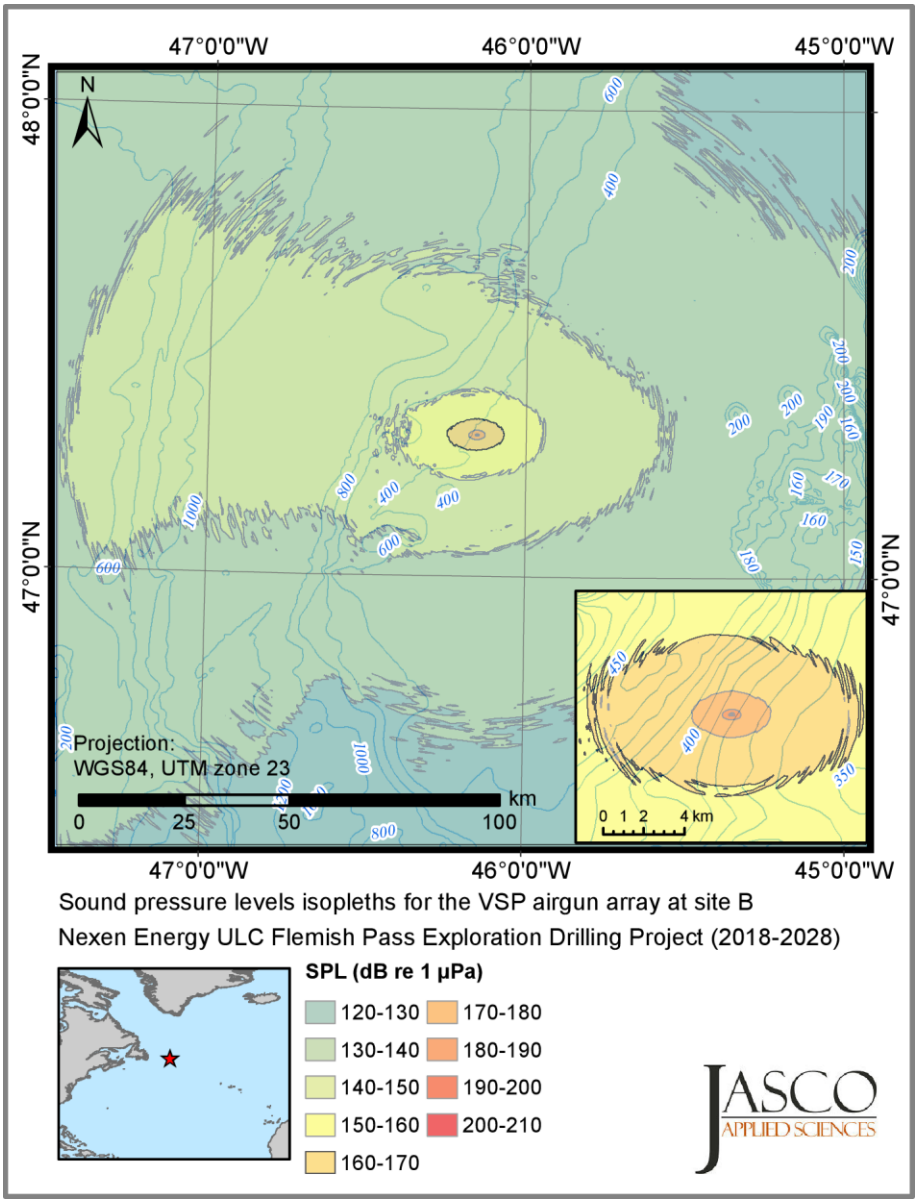

Figure 14. *Site B, VSP airgun array*: Broadband (10–25,000 Hz) maximum-over-depth SPL field. Blue contours indicate water depth in metres.

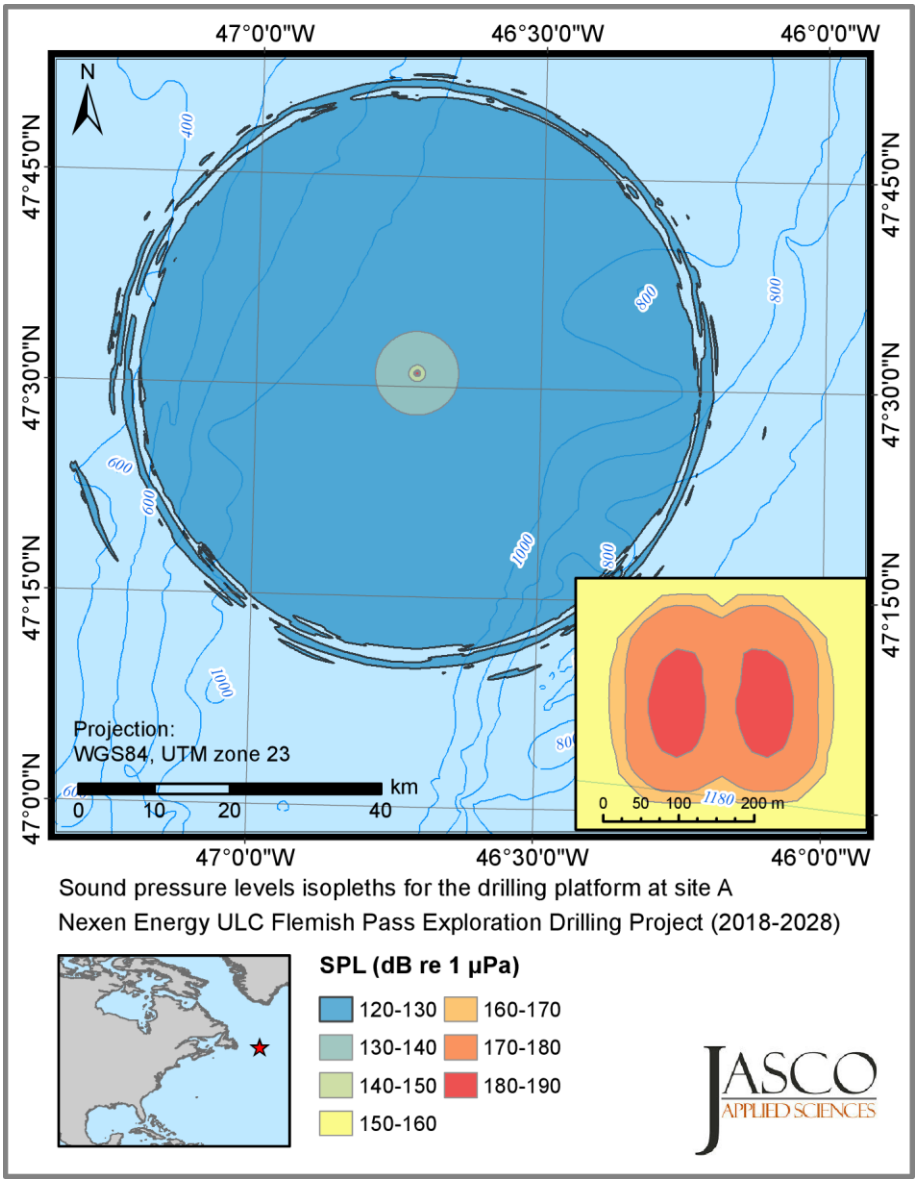

Figure 15. *Site A, Drilling platform*: Broadband (10–25,000 Hz) maximum-over-depth SPL field. Blue contours indicate water depth in metres.

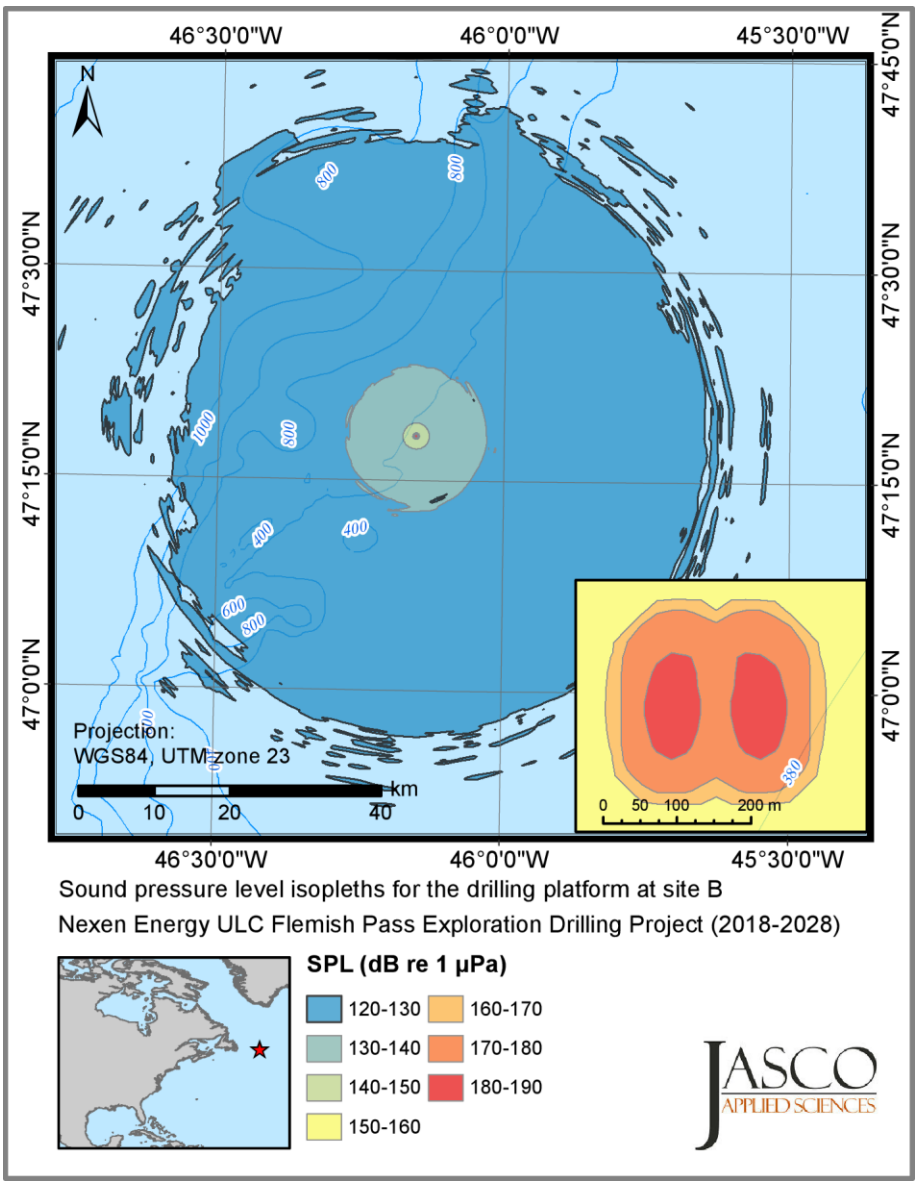

Figure 16. *Site B, Drilling platform*: Broadband (10–25,000 Hz) maximum-over-depth SPL field. Blue contours indicate water depth in metres.

4.2.2. Sound Exposure Levels (SEL)

Table 14 presents the distances to the M-weighted SEL_{24h} thresholds based on the injury criteria thresholds (listed in Table 2) for the VSP airgun array and the drilling platform, at the two modelling sites. Figures 17–20 present the associated sound fields as maximum-over-depth contour maps, showing the directivity and range to relevant M-weighted SEL_{24h} isopleths.

Table 14. Maximum (R_{max}) and 95% ($R_{95\%}$) horizontal distances (km) from the VSP airgun array and the centre of the drilling platform to modelled maximum-over-depth M-weighted 24 h sound exposure level thresholds (SEL_{24h}; dB re 1 $\mu Pa^2 \cdot s$).

Hearing group	VPS airgun array					Drilling platform				
	Threshold (dB re 1 $\mu Pa^2 \cdot s$)	Site A		Site B		Threshold (dB re 1 $\mu Pa^2 \cdot s$)	Site A		Site B	
		R_{max}	$R_{95\%}$	R_{max}	$R_{95\%}$		R_{max}	$R_{95\%}$	R_{max}	$R_{95\%}$
Low-frequency cetaceans	183	4.98	4.58	9.66	5.98	199	0.23	0.22	0.23	0.22
Mid-frequency cetaceans	185	-	-	-	-	198	0.18	0.16	0.18	0.16
High-frequency cetaceans	155	0.16	0.14	0.16	0.14	173	1.88	1.72	3.29	3.04
Phocid pinnipeds in water	185	0.38	0.34	0.38	0.34	201	0.16	0.15	0.16	0.15
Otariid pinnipeds in water	203	0.02	0.02	0.02	0.02	219	0.15	0.14	0.15	0.14

"-" symbol means the level was not reached.

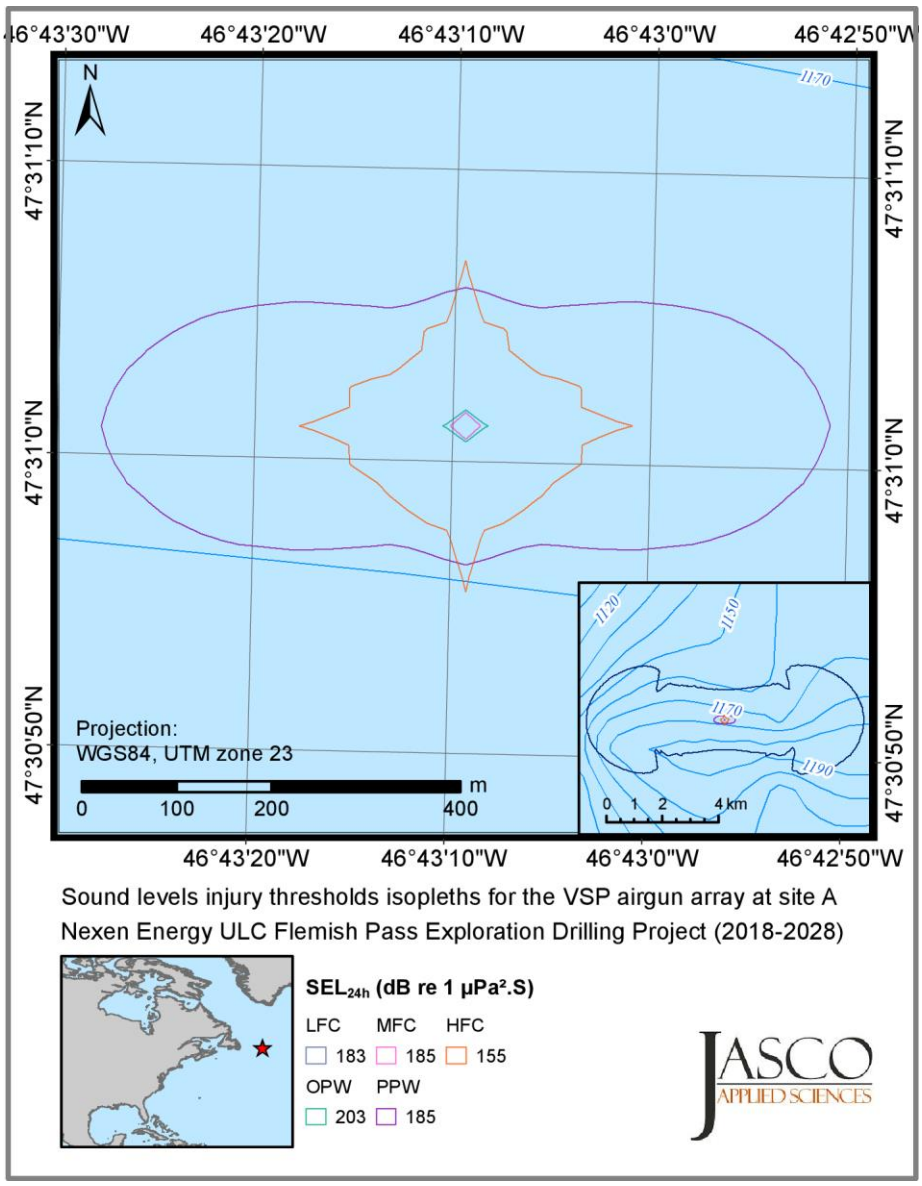

Figure 17. *Site A, VSP airgun array*: Broadband (10–25,000 Hz) maximum-over-depth M-weighted SEL_{24h} isopleths. Blue contours indicate water depth in metres.

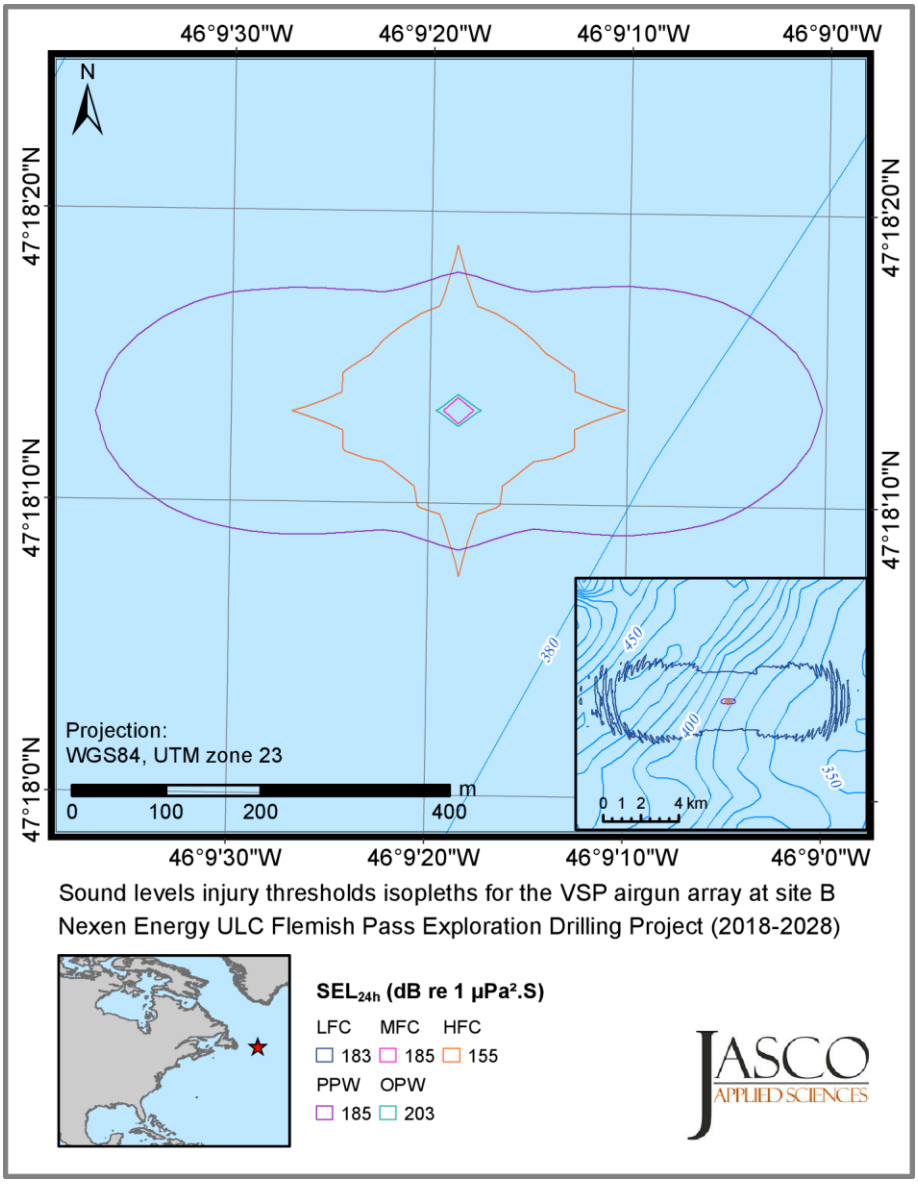

Figure 18. *Site B, VSP airgun array*: Broadband (10–25,000 Hz) maximum-over-depth M-weighted SEL_{24h} isopleths. Blue contours indicate water depth in metres.

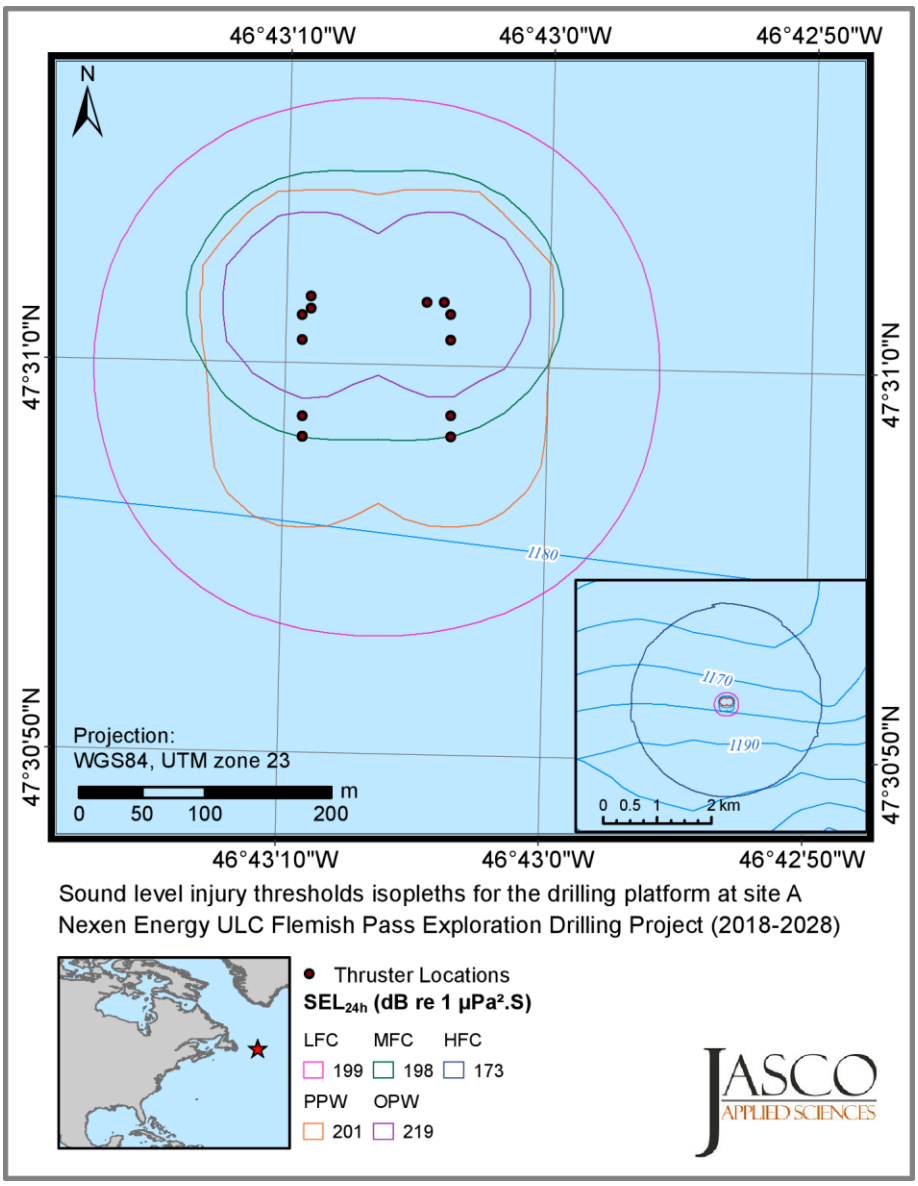

Figure 19. *Site A, Drilling platform*: Broadband (10–25,000 Hz) maximum-over-depth M-weighted SEL_{24h} isopleths. Blue contours indicate water depth in metres.

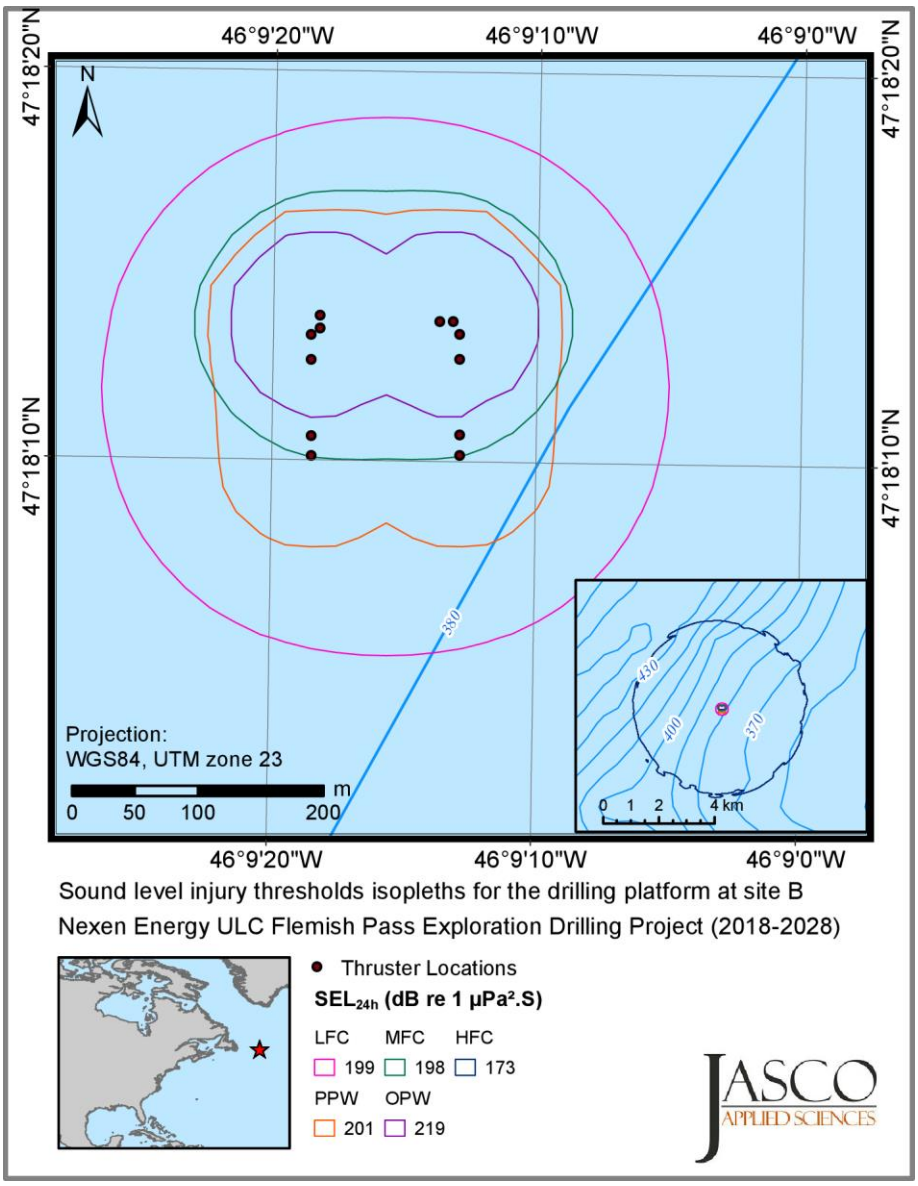

Figure 20. *Site B, Drilling platform*: Broadband (10–25,000 Hz) maximum-over-depth M-weighted SEL_{24h} isopleths. Blue contours indicate water depth in metres.

4.3. Ambient Levels

Ambient noise levels at the two JASCO recording stations (Figure 1; Section 3.4) were examined to document the local baseline underwater sound conditions. Monthly distributions provide an overview of the range of sound levels and how they change by season. To describe the general characteristics of the soundscape, ambient noise levels for four months throughout the year are presented as:

- Broadband and approximate-decade-band SPL over time for these frequency bands: 10 Hz to 4 kHz, 10–100 Hz, 100 Hz to 1 kHz, and 1–4 kHz. The associated graphs (Section 4.3.1) provide an overview of the time and frequency variations in the soundscape.
- Spectrograms: Ambient noise at each station was analyzed by Hamming-windowed fast Fourier transforms (FFTs), with 1 Hz resolution and 50% window overlap. The 120 FFTs performed with these settings are averaged to yield 1 min average spectra. These plots are presented with the SPL band plots (Section 4.3.1) and provide more detailed temporal and spectral distribution information that helps in indentifying the various noise contributors (e.g., marine mammals, and natural and geologic sources).
- Box-and-whisker plots[1] of the statistical distribution of SPL in each 1/3-octave frequency band. The boxes of the statistical distributions indicate the first (L_{25}), second (L_{50}), and third (L_{75}) quartiles. The whiskers (vertical lines) indicate the maximum and minimum range of the data. The solid line indicates the mean SPL, or L_{mean}, in each 1/3-octave frequency band. Theses plots are presented with the spectral density level percentile plots (Section 4.3.2).
- Spectral density level percentiles: Histograms of each frequency bin per 1 min of data. The L_{eq}, L_5, L_{25}, L_{50}, L_{75}, and L_{95} percentiles are plotted. The L_5 percentile curve is the frequency-dependent level exceeded by 5% of the 1 min averages. Equivalently, 95% of the 1 min spectral levels are above the 95th percentile curve. Theses curves (Section 4.3.2), together with the statistical distribution plots, provide information about the distribution of sound levels in each frequency band over a full month.
- Daily sound exposure levels (SEL): Computed for the total received sound energy and the detected shipping energy. The SEL is the linear sum of the 1 min SEL. For shipping, the 1 min SEL values are the linear 1 min squared SPL values multiplied by the duration, 60 s. For seismic survey pulses, the 1 min SEL is the linear sum of the per-pulse SEL. Although not frequency-filtered, these daily levels use the same sound metric as the injury criteria assessed in this report.

4.3.1. Ambient Sound Pressure Level versus Time

Long-term spectral averages along with median band-level time series figures (Figures 21–25) provide an overview of the time and frequency variations in the soundscape. Figure 21 presents the long-term spectrogram for the entire ESRF deployment running from July 2016 to July 2017. Station 18 noise levels remained fairly constant throughout the year, with the exception of an increase in noise levels in the 100–1000 Hz and 1–4 kHz bands in winter. This increase is attributed to wind-driven bubble and spray noise. The soundscape at Station 19 was strongly affected by seismic surveys in summer and fall, but mooring strum noise kept broadband noise levels high throughout the year. To represent the yearly temporal variations, Figures 22–26 show the SPL over February (2017), May (2017), August (2016), and November (2016). In February and May, the soundscape was influenced by vessel noise, particularly at Station 18, and flow noise around 25 Hz at Station 19. In August, the soundscape was dominated by seismic activity, but vessels continued to be important noise contributors at Station 18. Fin whale songs in the band of 18–25 Hz were detectable beginning in August, and were a dominant sound source from October through March at both stations.

[1] Box-and-whisker plots show groups of numerical data according to their quartiles. Vertical lines, or “whiskers”, extending vertically from the boxes indicate variability outside the upper and lower quartiles.

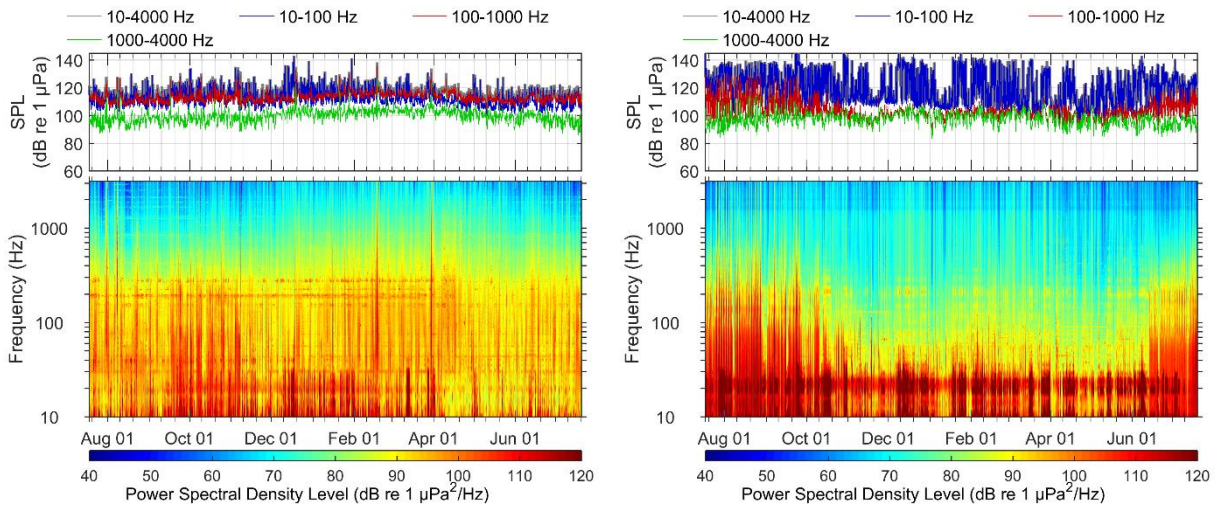

Figure 21. *July 2016 to July 2017*: Summary of acoustic data recorded at Station 18 (left) and 19 (right). For each station, the top figure is the median hourly in-band SPL and bottom is the long-term spectral average of the measured sound.

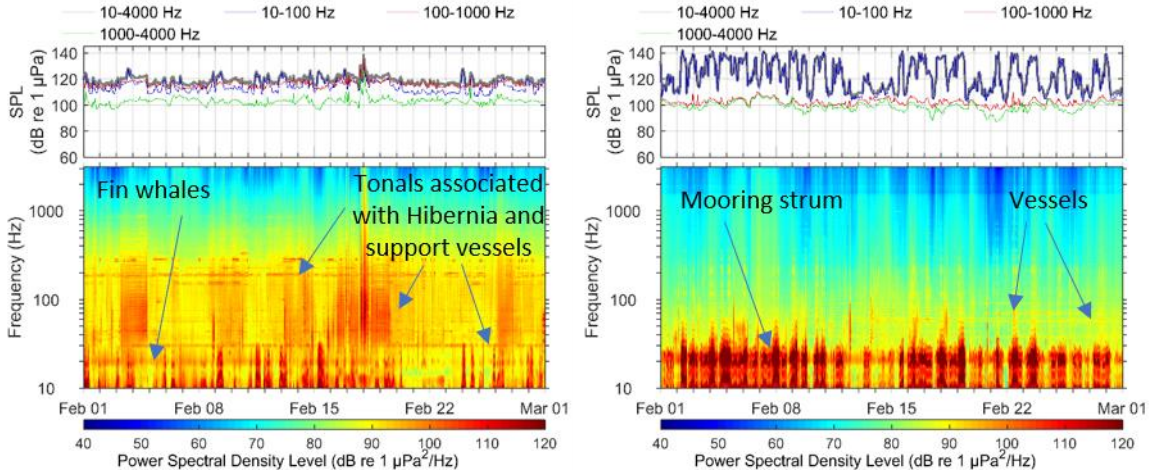

Figure 22. *February*: Summary of acoustic data recorded at Stations 18 (left) and 19 (right). For each station the top figure is the median hourly in-band SPL and bottom is the long-term spectral average of the measured sound.

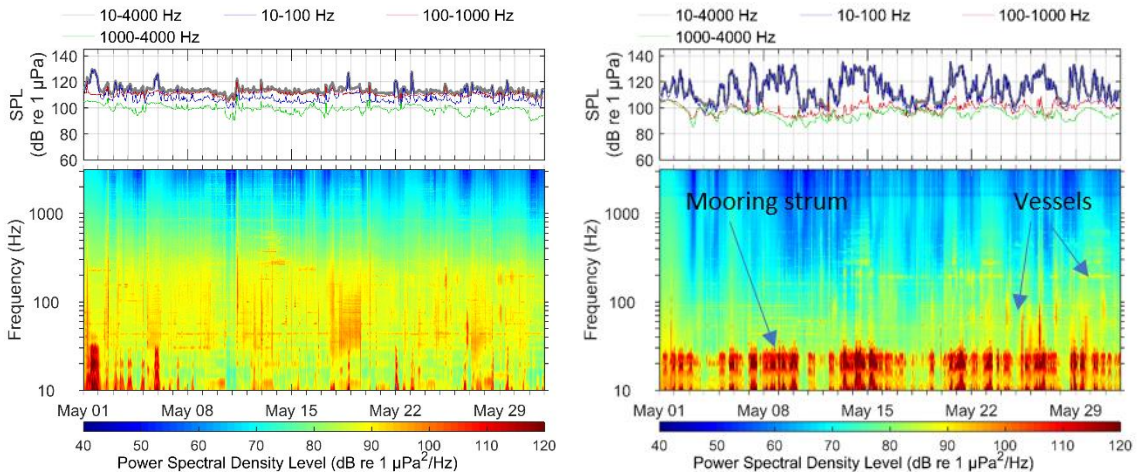

Figure 23. *May*: Summary of acoustic data recorded at Stations 18 (left) and 19 (right). For each station the top figure is the median hourly in-band SPL and bottom is the long-term spectral average of the measured sound.

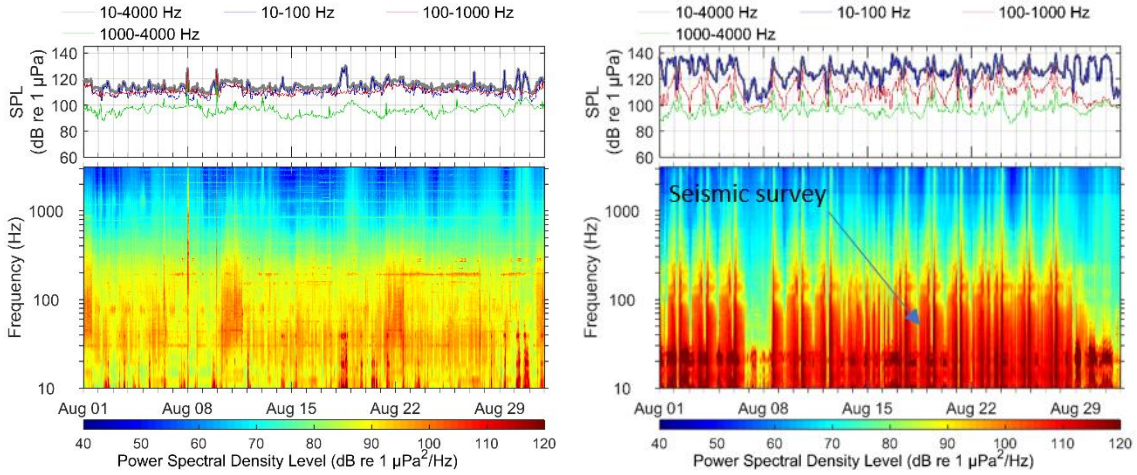

Figure 24. *August*: Summary of acoustic data recorded at Stations 18 (left) and 19 (right). For each station the top figure is the median hourly in-band SPL and bottom is the long-term spectral average of the measured sound.

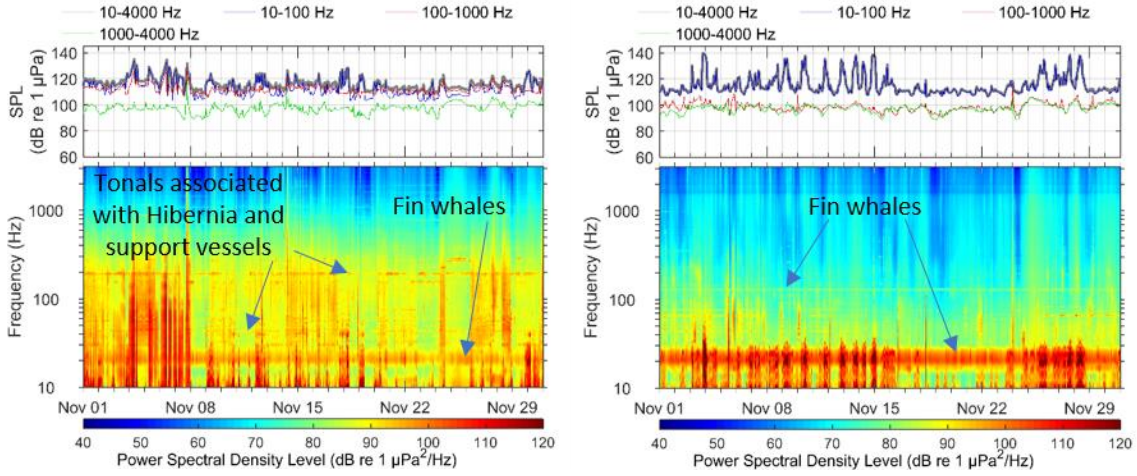

Figure 25. *November*: Summary of acoustic data recorded at Stations 18 (left) and 19 (right). For each station the top figure is the median hourly in-band SPL and bottom is the long-term spectral average of the measured sound.

4.3.2. Spectral Levels and 1/3-Octave Band Levels

Power spectral density and 1/3-octave-band distribution plots (Figures 26–29) can be directly compared to the Wenz plots (Figure 5) and provide more detailed spectral distribution information than the long-term spectral averages and box-and-whisker plots. The contribution of fin whale song notes at 20 and 130 Hz can be seen starting in August, peaking in November, and continuing until March. At Station 19, sound levels at 20–25 Hz were strongly influenced by flow noise, particularly in February and May. Seismic activity and shipping noise near Station 19 contributed to sound levels across a broad range of frequencies, raising the power spectrum levels by nearly 20 dB below 300 Hz. Note that the power spectral density levels were consistent across the band between months at Station 18, reflecting the steady activity and vessel traffic near the Hibernia platform.

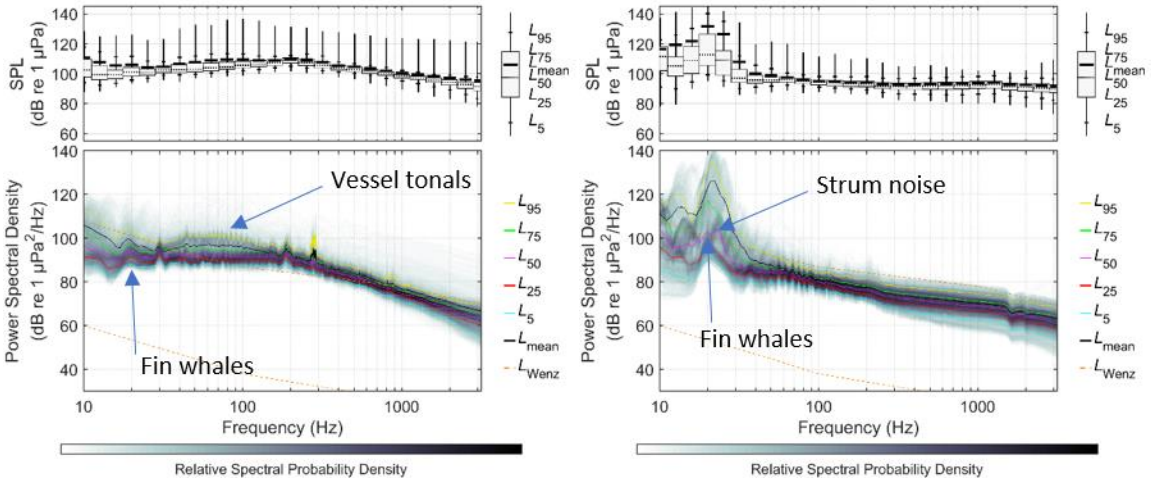

Figure 26. *February*: Summary of spectral content at Stations 18 (left) and 19 (right). For each station the top figure shows a box-and-whisker plot for the 1/3-octave-band SPL, and bottom shows the power spectral density percentiles and probability density (grayscale) of 1-min PSD levels compared to the limits of prevailing noise (Wenz 1962).

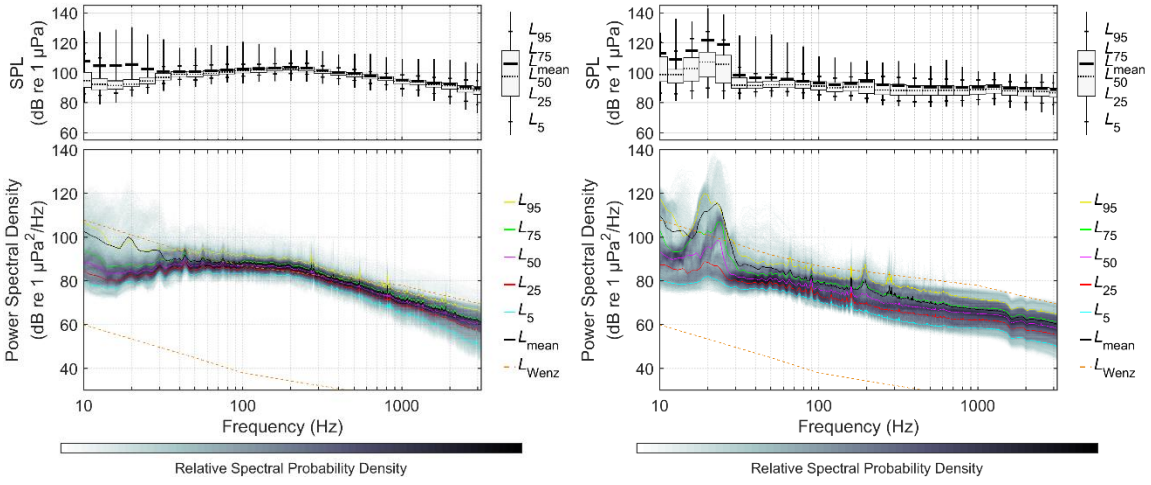

Figure 27. *May*: Summary of spectral content at Stations 18 (left) and 19 (right). For each station the top figure shows a box-and-whisker plot for the 1/3-octave-band SPL, and bottom shows the power spectral density percentiles and probability density (grayscale) of 1-min PSD levels compared to the limits of prevailing noise (Wenz 1962).

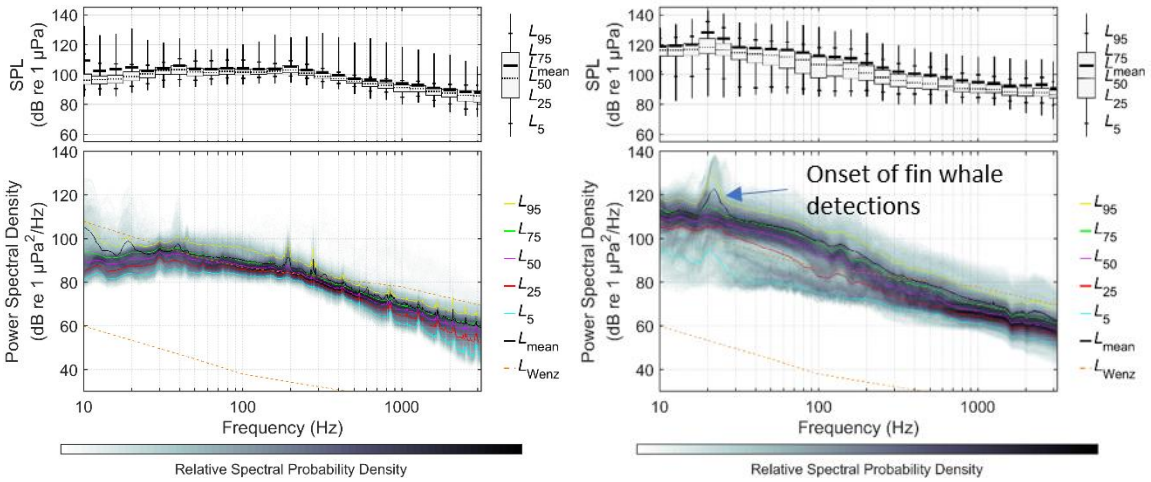

Figure 28. *August*: Summary of spectral content at Stations 18 (left) and 19 (right). For each station the top figure shows a box-and-whisker plot for the 1/3-octave-band SPL, and bottom shows the power spectral density percentiles and probability density (grayscale) of 1-min PSD levels compared to the limits of prevailing noise (Wenz 1962). The signatures of fin whales are annotated.

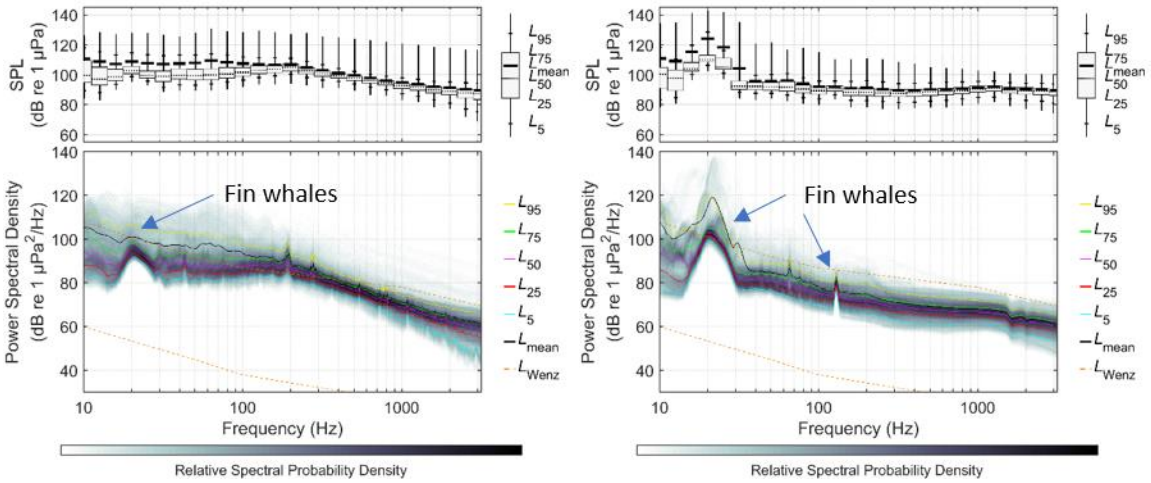

Figure 29. *November*: Summary of spectral content at Stations 18 (left) and 19 (right). For each station the top figure shows a box-and-whisker plot for the 1/3-octave-band SPL, and bottom shows the power spectral density percentiles and probability density (grayscale) of 1-min PSD levels compared to the limits of prevailing noise (Wenz 1962). The signatures of fin whales are annotated.

4.3.3. Daily Sound Exposure from Anthropogenic Sources

The daily SEL (Figures 30–33) integrates the total sound energy over 24 hours at a receiver location. SEL is one of the metrics used to define the thresholds for the onset of temporary and permanent threshold shifts (NMFS 2016). The presented ambient daily SEL are not, however, frequency-weighted and should not be directly compared to the thresholds in Table 2. Vessel activity was a primary noise contributor throughout the year, particularly at Station 18. Noise associated with seismic activity was not detected at either station in February. Among the four analyzed months, noise from seismic activities was only present at Station 19 in August, when it was the main contributor to the daily SEL. The contribution of anthropogenic sources decreased in November at Station 19, with peaks in daily SEL associated with current-induced mooring flow noise. Daily SEL were very consistent across months at Station 18, once again reflecting the steady ongoing activity at Hibernia. In contrast, SEL were lowest during winter at Station 19, when noise from shipping and seismic activity were at a minimum.

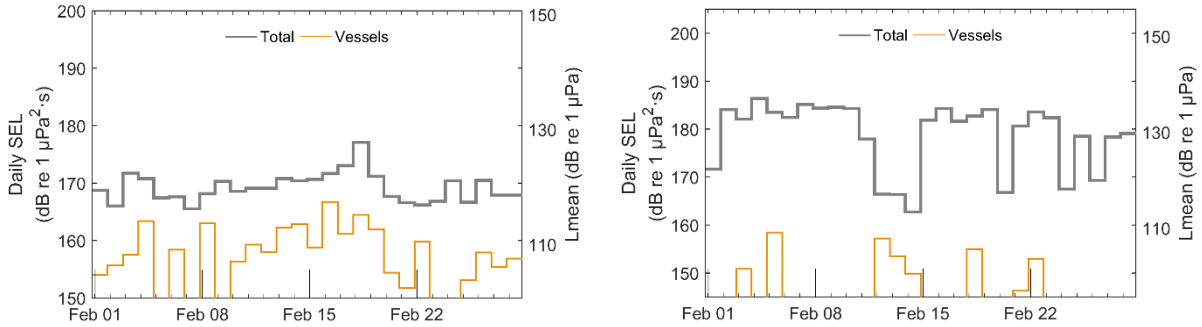

Figure 30. *February*: Total, vessel, and seismic-associated daily SEL and equivalent continuous noise levels (L_{mean}) at Stations 18 (left) and 19 (right).

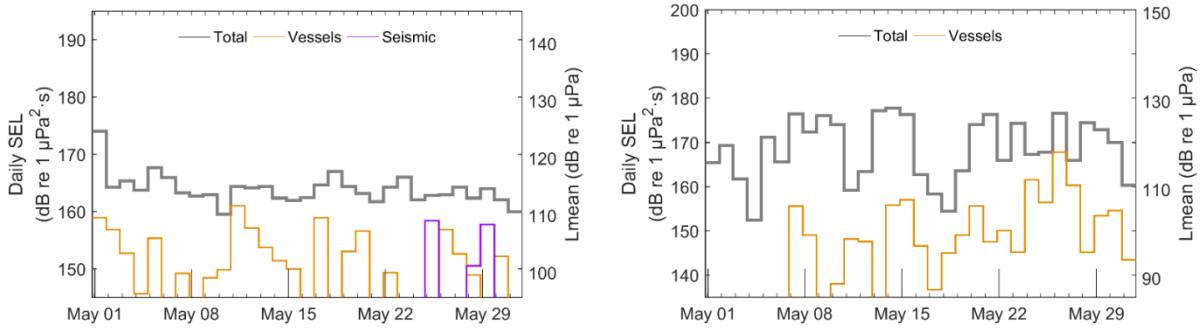

Figure 31. *May*: Total, vessel, and seismic-associated daily SEL and equivalent continuous noise levels (L_{mean}) at Stations 18 (left) and 19 (right).

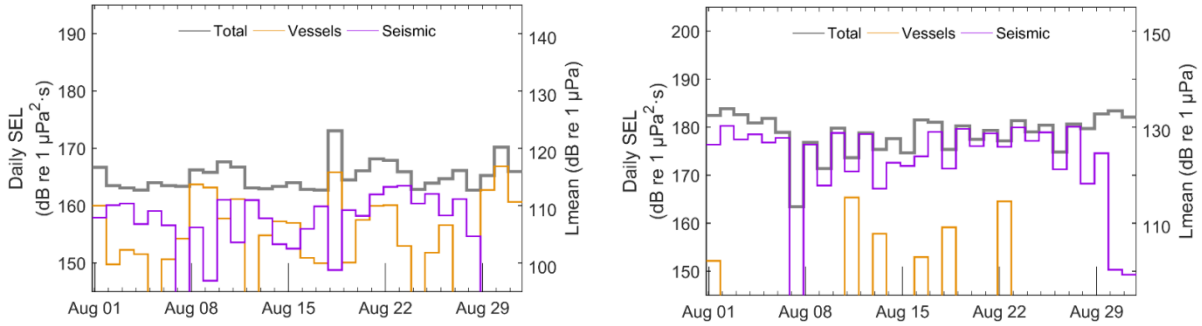

Figure 32. *August*: Total, vessel, and seismic-associated daily SEL and equivalent continuous noise levels (L_{mean}) at Stations 18 (left) and 19 (right).

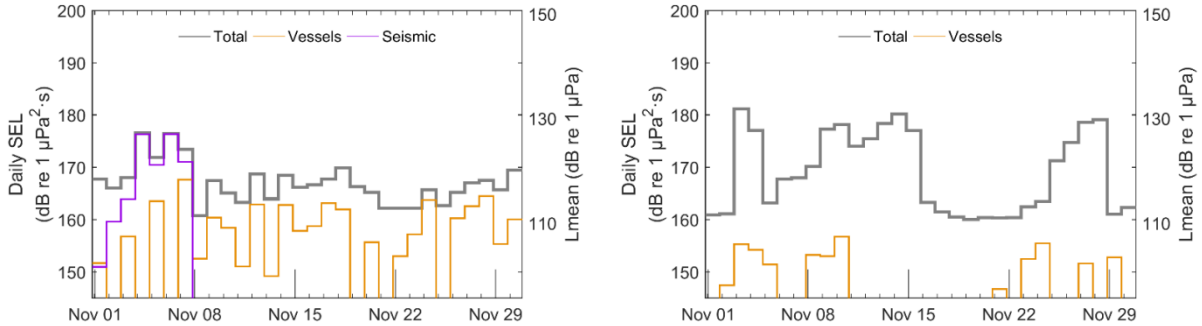

Figure 33. *November*: Total, vessel, and seismic-associated daily SEL and equivalent continuous noise levels (L_{mean}) at Stations 18 (left) and 19 (right).

5. Discussion

JASCO conducted a modelling study to estimate distances to underwater sound level thresholds associated with injury and behavioural to marine life during the Nexen Energy ULC Flemish Pass Exploration Drilling Project (2018–2028). Two scenarios were modelled: operation of a VSP airgun array and operation of a drilling platform. The assumption used throughout the modelling study (including the volume of the VSP airgun array, the number of VSP airgun array pulses in 24 h, and the choice of surrogates for the drilling platform) provide conservative estimates of the distances to marine mammal impact thresholds for the various activities that will occur during the Project.

Results show that distances to the various thresholds are generally longer at Site B (shallow site) than at Site A (deep site). Considering the injury criteria, the longest distances from VSP airgun array were for the low-frequency cetaceans (4.98 km at Site A and 9.66 km at Site B). From the drilling platform, the longest distances were for high-frequency cetaceans (1.88 km at Site A and 3.29 km at Site B). This difference in results is due to the difference in spectral levels between the two types of sources, as well as the difference in thresholds associated with the two types of sources (impulsive (VSP airgun array) versus non-impulsive (drilling platform)). Distances to all other injury thresholds were no longer than 380 m from the VSP airgun array and 228 m from the centre of the semi-submersible platform. Distances to behavioural threshold were 6.3–7.9 km for the VSP airgun array and 47.6–56.8 km for the drilling platforms.

Results were produced for May. Although distances to behavioural thresholds may be slightly longer for activities occurring from January to April, few activites are likely occur during this period because of heavy weather in the region. This reduction in antropogenic activity can be seen in the ambient levels recorded at the two JASCO stations (Section 4.3). Distance to injury criteria are much shorter and would not significantly vary throughout the year. Thus, the presented results are estimated to represent a conservative, yet a realistic assessment of the sound field throughout the operational period (2018–2028).

In February and May, the soundscape is influenced by vessel noise, particularly in regions closer to Newfoundland. In August, the soundscape is dominated by seismic activity and vessels. A previous JASCO study detected fin whale songs in August, and these songs were a dominant sound source from October through March, peaking in November.

Glossary

1/3-octave-band
Non-overlapping passbands that are one-third of an octave wide (where an octave is a doubling of frequency). Three adjacent 1/3-octave-bands comprise one octave. One-third-octave-bands become wider with increasing frequency. Also see octave.

A-weighting
Frequency-selective weighting for human hearing in air that is derived from the inverse of the idealized 40-phon equal loudness hearing function across frequencies.

absorption
The reduction of acoustic pressure amplitude due to acoustic particle motion energy converting to heat in the propagation medium.

ambient noise
All-encompassing sound at a given place, usually a composite of sound from many sources near and far (ANSI S1.1-1994 R2004), e.g., shipping vessels, seismic activity, precipitation, sea ice movement, wave action, and biological activity.

attenuation
The gradual loss of acoustic energy from absorption and scattering as sound propagates through a medium.

azimuth
A horizontal angle relative to a reference direction, which is often magnetic north or the direction of travel. In navigation it is also called bearing.

background noise
Total of all sources of interference in a system used for the production, detection, measurement, or recording of a signal, independent of the presence of the signal (ANSI S1.1-1994 R2004). Ambient noise detected, measured, or recorded with a signal is part of the background noise.

bandwidth
The range of frequencies over which a sound occurs. Broadband refers to a source that produces sound over a broad range of frequencies (e.g., seismic airguns, vessels) whereas narrowband sources produce sounds over a narrow frequency range (e.g., sonar) (ANSI/ASA S1.13-2005 R2010).

bar
Unit of pressure equal to 100 kPa, which is approximately equal to the atmospheric pressure on Earth at sea level. 1 bar is equal to 10^6 Pa or 10^{11} µPa.

broadband sound level
The total sound pressure level measured over a specified frequency range. If the frequency range is unspecified, it refers to the entire measured frequency range.

broadside direction
Perpendicular to the travel direction of a source. Compare with endfire direction.

cavitation
A rapid formation and collapse of vapor cavities (i.e., bubbles or voids) in water, most often caused by a rapid change in pressure. Fast-spinning vessel propellers typically cause cavitation, which creates a lot of noise.

cetacean
Any animal in the order Cetacea. These are aquatic, mostly marine mammals and include whales, dolphins, and porpoises.

compressional wave
A mechanical vibration wave in which the direction of particle motion is parallel to the direction of propagation. Also called primary wave or P-wave.

continuous sound
A sound whose sound pressure level remains above ambient sound during the observation period (ANSI/ASA S1.13-2005 R2010). A sound that gradually varies in intensity with time, for example, sound from a marine vessel.

decibel (dB)
One-tenth of a bel. Unit of level when the base of the logarithm is the tenth root of ten, and the quantities concerned are proportional to power (ANSI S1.1-1994 R2004).

endfire direction
Parallel to the travel direction of a source. See also broadside direction.

ensonified
Exposed to sound.

equal-loudness contour
A curve or curves that show, as a function of frequency, the sound pressure level required to cause a given loudness for a listener having normal hearing, listening to a specified kind of sound in a specified manner (ANSI S1.1-1994 R2004).

far-field
The zone where, to an observer, sound originating from an array of sources (or a spatially-distributed source) appears t o radiate from a single point. The distance to the acoustic far-field increases with frequency.

fast Fourier transform (FFT)
A computationally efficiently algorithm for computing the discrete Fourier transform.

frequency
The rate of oscillation of a periodic function measured in cycles-per-unit-time. The reciprocal of the period. Unit: hertz (Hz). Symbol: *f*. 1 Hz is equal to 1 cycle per second.

hearing group
Groups of marine mammal species with similar hearing ranges. Commonly defined functional hearing groups include low-, mid-, and high-frequency cetaceans, pinnipeds in water, and pinnipeds in air.

geoacoustic
Relating to the acoustic properties of the seabed.

hearing threshold
The sound pressure level for any frequency of the hearing group that is barely audible for a given individual in the absence of significant background noise during a specific percentage of experimental trials.

hertz (Hz)
A unit of frequency defined as one cycle per second.

high-frequency cetacean (HFC)
The functional cetacean hearing group that represents those odontocetes (toothed whales) specialized for hearing high frequencies.

intermittent sound
A level of sound that abruptly drops to the background noise level several times during the observation period.

impulsive sound
Sound that is typically brief and intermittent with rapid (within a few seconds) rise time and decay back to ambient levels (NOAA 2013, ANSI S12.7-1986 R2006). For example, seismic airguns and impact pile driving.

low-frequency cetacean (LFC)
The functional cetacean hearing group that represents mysticetes (baleen whales) specialized for hearing low frequencies.

median
The 50th percentile of a statistical distribution.

mid-frequency cetacean (MFC)
The functional cetacean hearing group that represents those odontocetes (toothed whales) specialized for mid-frequency hearing.

M-weighting
The process of band-pass filtering loud sounds to reduce the importance of inaudible or less-audible frequencies for broad classes of marine mammals. “Generalized frequency weightings for various functional hearing groups of marine mammals, allowing for their functional bandwidths and appropriate in characterizing auditory effects of strong sounds” (Southall et al. 2007).

mysticete
Mysticeti, a suborder of cetaceans, use their baleen plates, rather than teeth, to filter food from water. They are not known to echolocate, but use sound for communication. Members of this group include rorquals (Balaenopteridae), right whales (Balaenidae), and gray whales (*Eschrichtius robustus*).

non-impulsive sound
Sound that is broadband, narrowband or tonal, brief or prolonged, continuous or intermittent, and typically does not have a high peak pressure with rapid rise time (typically only small fluctuations in decibel level) that impulsive signals have (ANSI/ASA S3.20-1995 R2008). For example, marine vessels, aircraft, machinery, construction, and vibratory pile driving (NIOSH 1998, NOAA 2015).

octave
The interval between a sound and another sound with double or half the frequency. For example, one octave above 200 Hz is 400 Hz, and one octave below 200 Hz is 100 Hz.

otariid
A common term used to describe members of the Otariidae, eared seals, commonly called sea lions and fur seals. Otariids are adapted to a semi-aquatic life; they use their large fore flippers for propulsion. Their ears distinguish them from phocids. Otariids are one of the three main groups in the superfamily Pinnipedia; the other two groups are phocids and walrus.

otariid pinnipeds in water (OPW)
The functional pinniped hearing group that represents eared seals.

parabolic equation method
A computationally-efficient solution to the acoustic wave equation that is used to model transmission loss. The parabolic equation approximation omits effects of back-scattered sound, simplifying the computation of transmission loss. The effect of back-scattered sound is negligible for most ocean-acoustic propagation problems.

peak pressure level (PK)
The maximum instantaneous sound pressure level, in a stated frequency band, within a stated period. Also called zero-to-peak pressure level. Unit: decibel (dB).

peak-to-peak pressure level (PK-PK)
The difference between the maximum and minimum instantaneous pressure levels. Unit: decibel (dB).

percentile level, exceedance
The sound level exceeded *n* % of the time during a measurement.

permanent threshold shift (PTS)
A permanent loss of hearing sensitivity caused by excessive noise exposure. PTS is considered auditory injury.

phocid
A common term used to describe all members of the family Phocidae. These true/earless seals are more adapted to in-water life than are otariids, which have more terrestrial adaptations. Phocids use their hind flippers to propel themselves. Phocids are one of the three main groups in the superfamily Pinnipedia; the other two groups are otariids and walrus.

phocid pinnipeds in water (PPW)
The functional pinniped hearing group that represents true/earless seals.

pinniped
A common term used to describe all three groups that form the superfamily Pinnipedia: phocids (true seals or earless seals), otariids (eared seals or fur seals and sea lions), and walrus.

point source
A source that radiates sound as if from a single point (ANSI S1.1-1994 R2004).

power spectrum density
The acoustic signal power per unit frequency as measured at a single frequency. Unit: $\mu Pa^2/Hz$, or $\mu Pa^2 \cdot s$.

power spectral density level
The decibel level ($10\log_{10}$) of the power spectrum density, usually presented in 1 Hz bins. Unit: dB re 1 $\mu Pa^2/Hz$.

pressure, acoustic
The deviation from the ambient hydrostatic pressure caused by a sound wave. Also called overpressure. Unit: pascal (Pa). Symbol: *p*.

pressure, hydrostatic
The pressure at any given depth in a static liquid that is the result of the weight of the liquid acting on a unit area at that depth, plus any pressure acting on the surface of the liquid. Unit: pascal (Pa).

received level
The sound level measured at a receiver.

rms
root-mean-square.

shear wave
A mechanical vibration wave in which the direction of particle motion is perpendicular to the direction of propagation. Also called secondary wave or S-wave. Shear waves propagate only in solid media, such as sediments or rock. Shear waves in the seabed can be converted to compressional waves in water at the water-seabed interface.

signature
Pressure signal generated by a source.

sound
A time-varying pressure disturbance generated by mechanical vibration waves travelling through a fluid medium such as air or water.

sound exposure
Time integral of squared, instantaneous frequency-weighted sound pressure over a stated time interval or event. Unit: pascal-squared second ($Pa^2 \cdot s$) (ANSI S1.1-1994 R2004).

sound exposure level (SEL)
A cumulative measure related to the sound energy in one or more pulses. Unit: dB re 1 $\mu Pa^2 \cdot s$. SEL is expressed over the summation period (e.g., per-pulse SEL [for airguns], single-strike SEL [for pile drivers], 24-hour SEL).

sound field
Region containing sound waves (ANSI S1.1-1994 R2004).

sound intensity
Sound energy flowing through a unit area perpendicular to the direction of propagation per unit time.

sound pressure level (SPL)
The decibel ratio of the time-mean-square sound pressure, in a stated frequency band, to the square of the reference sound pressure (ANSI S1.1-1994 R2004).

For sound in water, the reference sound pressure is one micropascal (p_0 = 1 µPa) and the unit for SPL is dB re 1 µPa:

$$\mathrm{SPL} = 10\log_{10}\left(p^2 / p_0^2\right) = 20\log_{10}\left(p / p_0\right)$$

Unless otherwise stated, SPL refers to the root-mean-square sound pressure level. See also 90% sound pressure level and fast-average sound pressure level. Non-rectangular time window functions may be applied during calculation of the rms value, in which case the SPL unit should identify the window type.

sound speed profile
The speed of sound in the water column as a function of depth below the water surface.

source level (SL)
The sound level measured in the far-field and scaled back to a standard reference distance of 1 metre from the acoustic centre of the source. Unit: dB re 1 µPa @ 1 m (sound pressure level) or dB re 1 $\mu Pa^2 \cdot s$ (sound exposure level).

spectrogram
A visual representation of acoustic amplitude compared with time and frequency.

spectrum
An acoustic signal represented in terms of its power (or energy) distribution compared with frequency.

temporary threshold shift (TTS)
Temporary loss of hearing sensitivity caused by excessive noise exposure.

transmission loss (TL)
The decibel reduction in sound level between two stated points that results from sound spreading away from an acoustic source subject to the influence of the surrounding environment. Also called propagation loss.

wavelength
Distance over which a wave completes one oscillation cycle. Unit: meter (m). Symbol: λ.

Literature Cited

[HESS] High Energy Seismic Survey. 1999. *High Energy Seismic Survey Review Process and Interim Operational Guidelines for Marine Surveys Offshore Southern California*. Prepared for the California State Lands Commission and the United States Minerals Management Service Pacific Outer Continental Shelf Region by the High Energy Seismic Survey Team, Camarillo, California. 98 pp.

[ISO] International Organization for Standardization. 2016. *ISO/DIS 18405.2:2017. Underwater acoustics—Terminology*. Geneva. https://www.iso.org/standard/62406.html.

[MMC] Marine Mammal Commission. 2007. *Marine mammals and noise: A sound approach to research and management*. A Report to Congress from the Marine Mammal Commission. http://www.mmc.gov/reports/workshop/pdf/fullsoundreport.pdf.

[NIOSH] National Institute for Occupational Safety and Health. 1998. *Criteria for a recommended standard: Occupational noise exposure*. Document Number 98-126. U.S. Department of Health and Human Services, NIOSH, Cincinnati, Ohio. 122 pp.

[NMFS] National Marine Fisheries Service. 1998. *Acoustic Criteria Workshop*. Dr. Roger Gentry and Dr. Jeanette Thomas Co-Chairs.

[NMFS] National Marine Fisheries Service. 2013. *Marine Mammals: Interim Sound Threshold Guidance* (webpage). National Marine Fisheries Service, National Oceanic and Atmospheric Administration, U.S. Department of Commerce. http://www.westcoast.fisheries.noaa.gov/protected_species/marine_mammals/threshold_guidance.html.

[NMFS] National Marine Fisheries Service. 2016. *Technical Guidance for Assessing the Effects of Anthropogenic Sound on Marine Mammal Hearing: Underwater Acoustic Thresholds for Onset of Permanent and Temporary Threshold Shifts*. U.S. Department of Commerce, NOAA. NOAA Technical Memorandum NMFS-OPR-55. 178 pp. http://www.nmfs.noaa.gov/pr/acoustics/Acoustic%20Guidance%20Files/opr-55_acoustic_guidance_tech_memo.pdf.

[NOAA] National Oceanic and Atmospheric Administration. 2013. *Draft guidance for assessing the effects of anthropogenic sound on marine mammals: Acoustic threshold levels for onset of permanent and temporary threshold shifts*, December 2013, 76 pp. Silver Spring, Maryland: NMFS Office of Protected Resources. http://www.nmfs.noaa.gov/pr/acoustics/draft_acoustic_guidance_2013.pdf.

[NOAA] National Oceanic and Atmospheric Administration. 2015. *Draft guidance for assessing the effects of anthropogenic sound on marine mammal hearing: Underwater acoustic threshold levels for onset of permanent and temporary threshold shifts*, July 2015, 180 pp. Silver Spring, Maryland: NMFS Office of Protected Resources. http://www.nmfs.noaa.gov/pr/acoustics/draft%20acoustic%20guidance%20July%202015.pdf.

[NOAA] National Oceanic and Atmospheric Administration. 2016. *Document Containing Proposed Changes to the NOAA Draft Guidance for Assessing the Effects of Anthropogenic Sound on Marine Mammal Hearing: Underwater Acoustic Threshold Levels for Onset of Permanent and Temporary Threshold Shifts*, p. 24. http://www.nmfs.noaa.gov/pr/acoustics/draft_guidance_march_2016_.pdf.

[NRC] National Research Council. 2003. *Ocean Noise and Marine Mammals*. National Research Council (U.S.), Ocean Studies Board, Committee on Potential Impacts of Ambient Noise in the Ocean on

Marine Mammals. The National Academies Press, Washington, DC. 192 pp. http://www.nap.edu/openbook.php?record_id=10564.

[ONR] Office of Naval Research. 1998. *ONR Workshop on the Effect of Anthropogenic Noise in the Marine Environment*. Dr. R. Gisiner Chair.

Aerts, L., M. Blees, S. Blackwell, C. Greene, K. Kim, D. Hannay, and M. Austin. 2008. *Marine mammal monitoring and mitigation during BP Liberty OBC seismic survey in Foggy Island Bay, Beaufort Sea, July-August 2008: 90-day report*. Document Number LGL Report P1011-1. Report by LGL Alaska Research Associates Inc., LGL Ltd., Greeneridge Sciences Inc. and JASCO Applied Sciences for BP Exploration Alaska. 199 pp. http://www.nmfs.noaa.gov/pr/pdfs/permits/bp_liberty_monitoring.pdf.

ANSI S12.7-1986. R2006. *American National Standard Methods for Measurements of Impulsive Noise*. American National Standards Institute, New York.

ANSI S1.1-1994. R2004. *American National Standard Acoustical Terminology*. American National Standards Institute, New York.

ANSI S1.1-2013. R2013. *American National Standard Acoustical Terminology*. American National Standards Institute, New York.

ANSI/ASA S1.13-2005. R2010. *American National Standard Measurement of Sound Pressure Levels in Air*. American National Standards Institute and Acoustical Society of America, New York.

ANSI/ASA S3.20-1995. R2008. *American National Standard Bioacoustical Terminology*. American National Standards Institute and Acoustical Society of America, New York.

Babushina, Y.S., G.L. Zaslavskii, and L.I. Yurkevich. 1991. Air and underwater hearing characteristics of the northern fur seal: Audiograms, frequency and differential thresholds. *Biophysics* 39: 900-913.

Brown, N.A. 1977. Cavitation noise problems and solutions. *Proceedings International Symposium on Shipboard Acoustics*: 18.

Buckingham, M.J. 2005. Compressional and shear wave properties of marine sediments: Comparisons between theory and data. *Journal of the Acoustical Society of America* 117(1): 137-152.

Burdic, W.S. 1984. *Underwater acoustic system analysis*. 1st edition. Prentice Hall, Englewood Cliffs, NJ. 445.

Carnes, M.R. 2009. *Description and Evaluation of GDEM-V 3.0*. Document Number NRL Memorandum Report 7330-09-9165. US Naval Research Laboratory, Stennis Space Center, MS. 21 pp.

Collins, M.D. 1993. A split-step Padé solution for the parabolic equation method. *Journal of the Acoustical Society of America* 93(4): 1736-1742.

Collins, M.D., R.J. Cederberg, D.B. King, and S. Chin-Bing. 1996. Comparison of algorithms for solving parabolic wave equations. *Journal of the Acoustical Society of America* 100(1): 178-182.

Coppens, A.B. 1981. Simple equations for the speed of sound in Neptunian waters. *Journal of the Acoustical Society of America* 69(3): 862-863. http://link.aip.org/link/?JAS/69/862/1.

Deane, G.B. 2000. Long time-base observations of surf noise. *Journal of the Acoustical Society of America* 107(2): 758-770.

Dragoset, W.H. 1984. A comprehensive method for evaluating the design of airguns and airgun arrays. *Proceedings, 16th Annual Offshore Technology Conference* Volume 3, May 7-9, 1984. OTC 4747, Houston, Houston. 75–84 pp.

Ellison, W.T. and P.J. Stein. 1999. *SURTASS LFA High Frequency Marine Mammal Monitoring (HF/M3) Sonar: Sustem Description and Test & Evaluation*. Under U.S. Navy Contract N66604-98-D-5725.

Finneran, J.J. and C.E. Schlundt. 2010. Frequency-dependent and longitudinal changes in noise-induced hearing loss in a bottlenose dolphin (*Tursiops truncatus*). *Journal of the Acoustical Society of America* 128(2): 567-570.

Finneran, J.J. and A.K. Jenkins. 2012. *Criteria and thresholds for U.S. Navy acoustic and explosive effects analysis*. SPAWAR Systems Center Pacific, San Diego, California.

Finneran, J.J. 2015. *Auditory weighting functions and TTS/PTS exposure functions for cetaceans and marine carnivores*. San Diego: SSC Pacific.

Finneran, J.J. 2016. *Auditory weighting functions and TTS/PTS exposure functions for marine mammals exposed to underwater noise*. Technical Report. 49 pp.

Fisher, F.H. and V.P. Simmons. 1977. Sound absorption in sea water. *Journal of the Acoustical Society of America* 62(3): 558-564. http://link.aip.org/link/?JAS/62/558/1.

Fletcher, J.L. and R.G. Busnel. 1978. *Effects of noise on wildlife*. Academic Press, New York.

Funk, D., D. Hannay, D. Ireland, R. Rodrigues, and W. Koski (eds.). 2008. *Marine mammal monitoring and mitigation during open water seismic exploration by Shell Offshore Inc. in the Chukchi and Beaufort Seas, July–November 2007: 90-day report*. LGL Report P969-1. Prepared by LGL Alaska Research Associates Inc., LGL Ltd., and JASCO Research Ltd. for Shell Offshore Inc., National Marine Fisheries Service (US), and US Fish and Wildlife Service. 218 pp.

Hannay, D. and R. Racca. 2005. *Acoustic Model Validation*. Document Number 0000-S-90-04-T-7006-00-E, Revision 02. Technical report for Sakhalin Energy Investment Company Ltd. by JASCO Research Ltd. 34 pp.

Huppertz, T.J. 2007. *Late Quaternary History of Flemich Pass, Southeast Canadian Continental Margin*. M.Sc. Thesis. Dalhousie University, Halifax, Nova Scotia. 137 pp.

Ireland, D.S., R. Rodrigues, D. Funk, W. Koski, and D. Hannay. 2009. *Marine mammal monitoring and mitigation during open water seismic exploration by Shell Offshore Inc. in the Chukchi and Beaufort Seas, July–October 2008: 90-Day Report*. Document Number LGL Report P1049-1. 277 pp.

Kastak, D. and R.J. Schusterman. 1998. Low-frequency amphibious hearing in pinnipeds: Methods, measurements, noise, and ecology. *Journal of the Acoustical Society of America* 103: 2216-2228.

Kastelein, R.A., R. van Schie, W.C. Verboom, and D. de Haan. 2005. Underwater hearing sensitivity of a male and a female Steller sea lion (*Eumetopias jubatus*). *Journal of the Acoustical Society of America* 118(3): 1820-1829.

Landro, M. 1992. Modeling of GI gun signatures. *Geophysical Prospecting* 40: 721–747.

Laws, M., L. Hatton, and M. Haartsen. 1990. Computer modeling of clustered airguns. *First Break* 8: 331–338.

Leggat, L.J., H.M. Merklinger, and J.L. Kennedy. 1981. *LNG Carrier Underwater Noise Study for Baffin Bay*. Defence Research Establishment Atlantic, Dartmouth, Nova Scotia. 32 pp.

Lucke, K., U. Siebert, P. Lepper, A., and M.-A. Blanchet. 2009. Temporary shift in masked hearing thresholds in a harbor porpoise (*Phocoena phocoena*) after exposure to seismic airgun stimuli. *Journal of the Acoustical Society of America* 125(6): 4060-4070.

Lurton, X. 2002. *An Introduction to Underwater Acoustics: Principles and Applications*. Springer, Chichester, U.K. 347.

MacGillivray, A.O. 2006. *Acoustic Modelling Study of Seismic Airgun Noise in Queen Charlotte Basin*. MSc Thesis. University of Victoria, Victoria, BC. 98 pp.

MacGillivray, A.O. and N.R. Chapman. 2012. Modeling underwater sound propagation from an airgun array using the parabolic equation method. *Canadian Acoustics* 40(1): 19-25. http://jcaa.caa-aca.ca/index.php/jcaa/article/view/2502.

Malme, C.I., P.R. Miles, C.W. Clark, P. Tyak, and J.E. Bird. 1983. *Investigations of the Potential Effects of Underwater Noise from Petroleum Industry Activities on Migrating Gray Whale Behavior*. Report Number 5366. http://www.boem.gov/BOEM-Newsroom/Library/Publications/1983/rpt5366.aspx.

Malme, C.I., P.R. Miles, C.W. Clark, P. Tyack, and J.E. Bird. 1984. *Investigations of the potential effects of underwater noise from petroleum industry activities on migrating gray whale behavior. Phase II: January 1984 migration*. Report Number BBN Report 5586. Bolt Beranek and Newman Inc. 357 pp.

Martin, B., K. Broker, M.-N.R. Matthews, J. MacDonnell, and L. Bailey. 2015. *Comparison of measured and modeled air-gun array sound levels in Baffin Bay, West Greenland. OceanNoise 2015*, 11-15 May, Barcelona, Spain.

Martin, S.B., M.-N.R. Matthews, J.T. MacDonnell, and K. Bröker. 2017. Characteristics of seismic survey pulses and the ambient soundscape in Baffin Bay and Melville Bay, West Greenland. *Journal of the Acoustic Society of America* 142(3331). https://doi.org/10.1121/1.5014049.

Mattsson, A. and M. Jenkerson. 2008. *Single Airgun and Cluster Measurement Project*. *Joint Industry Programme (JIP) on Exploration and Production Sound and Marine Life Proramme Review*, October 28-30. International Association of Oil and Gas Producers, Houston, TX.

Moore, P.W.B. and R.J. Schusterman. 1987. Audiometric assessment of northern fur seals, *Callorhinus ursinus*. *Marine Mammal Science* 3: 31-53.

Mulsow, J. and C. Reichmuth. 2007. Electrophysiological assessment of temporal resolution in pinnipeds. *Aquatic Mammals* 33: 122-131.

Mulsow, J., J.J. Finneran, and D.S. Houser. 2011a. California sea lion (*Zalophus californianus*) aerial hearing sensitivity measured using auditory steady-state response and psychophysical methods. *Journal of the Acoustical Society of America* 129: 2298-2306.

Mulsow, J., C. Reichmuth, F.M.D. Gulland, D.A.S. Rosen, and J.J. Finneran. 2011b. Aerial audiograms of several California sea lions (*Zalophus californianus*) and Steller sea lions (*Eumetopias jubatus*) measured using single and multiple simultaneous auditory steady-state response methods. *Journal of Experimental Biology* 214: 1138-1147.

Nedwell, J.R. and A.W. Turnpenny. 1998. The use of a generic frequency weighting scale in estimating environmental effect. *Workshop on Seismics and Marine Mammals*. 23–25th June 1998, London, U.K.

Nedwell, J.R., A.W.H. Turnpenny, J. Lovell, S.J. Parvin, R. Workman, and J.A.L. Spinks. 2007. *A validation of the dB_{ht} as a measure of the behavioural and auditory effects of underwater noise*. Report No. 534R1231 prepared by Subacoustech Ltd. for the UK Department of Business, Enterprise and Regulatory Reform under Project No. RDCZ/011/0004. www.subacoustech.com/information/downloads/reports/534R1231.pdf.

Nowacek, D.P., L.H. Thorne, D.W. Johnston, and P.L. Tyack. 2007. Responses of cetaceans to anthropogenic noise. *Mammal Review* 37(2): 81-115.

O'Neill, C., D. Leary, and A. McCrodan. 2010. Sound Source Verification. (Chapter 3) *In* Blees, M.K., K.G. Hartin, D.S. Ireland, and D. Hannay (eds.). *Marine mammal monitoring and mitigation during open water seismic exploration by Statoil USA E&P Inc. in the Chukchi Sea, August-October 2010: 90-day report*. LGL Report P1119. Prepared by LGL Alaska Research Associates Inc., LGL Ltd., and JASCO Applied Sciences Ltd. for Statoil USA E&P Inc., National Marine Fisheries Service (US), and US Fish and Wildlife Service. 1-34.

Payne, R. and D. Webb. 1971. Orientation by means of long range acoustic signaling in baleen whales. *Annals of the New York Academy of Sciences* 188: 110-142.

Porter, M.B. and Y.-C. Liu. 1994. Finite-element ray tracing. *In*: Lee, D. and M.H. Schultz (eds.). *Proceedings of the International Conference on Theoretical and Computational Acoustics*. Volume 2. World Scientific Publishing Co. 947-956 pp.

Racca, R., A. Rutenko, K. Bröker, and M. Austin. 2012a. A line in the water - design and enactment of a closed loop, model based sound level boundary estimation strategy for mitigation of behavioural impacts from a seismic survey. *11th European Conference on Underwater Acoustics 2012*. Volume 34(3), Edinburgh, United Kingdom.

Racca, R., A. Rutenko, K. Bröker, and G. Gailey. 2012b. *Model based sound level estimation and in-field adjustment for real-time mitigation of behavioural impacts from a seismic survey and post-event evaluation of sound exposure for individual whales*. *Acoustics 2012 Fremantle: Acoustics, Development and the Environment*, Fremantle, Australia. http://www.acoustics.asn.au/conference_proceedings/AAS2012/papers/p92.pdf.

Richardson, W.J., B. Würsig, and C.R. Greene, Jr. 1986. Reactions of bowhead whales, *Balaena mysticetus*, to seismic exploration in the Canadian Beaufort Sea. *Journal of the Acoustical Society of America* 79(4): 1117-1128.

Richardson, W.J., B. Würsig, and C.R. Greene, Jr. 1990. Reactions of bowhead whales, *Balaena mysticetus*, to drilling and dredging noise in the Canadian Beaufort Sea. *Marine Environmental Research* 29(2): 135-160. http://www.sciencedirect.com/science/article/pii/014111369090032J.

Richardson, W.J., C.R. Greene, Jr., C.I. Malme, and D.H. Thomson. 1995. *Marine Mammals and Noise*. Academic Press, San Diego, California. 576.

Rodríguez, E., C.S. Morris, Y.J.E. Belz, E.C. Chapin, J.M. Martin, W. Daffer, and S. Hensley. 2005. *An Assessment of the SRTM Topographic Products*. Document Number JPL D-31639. Jet Propulsion Laboratory, Pasadena, CA.

Ross, D. 1976. *Mechanics of Underwater Noise*. Pergamon Press, New York. 375 pp.

Schusterman, R.J., R.F. Balliet, and J. Nixon. 1972. Underwater audiogram of the California sea lion by the conditioned vocalization technique. *Journal of the Experimental Analysis of Behavior* 17: 339-350.

Shipboard Scientific Party. 1994. *Site 905, Leg 150*. *In*: Mountain, G.S., K.G. Miller, P. Blum, and et al. (eds.). Deep Sea Drilling Projects Initial Reports. 255–308 pp. http://www.deepseadrilling.org/96/volume/dsdp96_16.pdf.

Southall, B.L., A.E. Bowles, W.T. Ellison, J.J. Finneran, R.L. Gentry, C.R. Greene, Jr., D. Kastak, D.R. Ketten, J.H. Miller, et al. 2007. Marine mammal noise exposure criteria: Initial scientific recommendations. *Aquatic Mammals* 33(4): 411-521.

Teague, W.J., M.J. Carron, and P.J. Hogan. 1990. A comparison between the Generalized Digital Environmental Model and Levitus climatologies. *Journal of Geophysical Research* 95(C5): 7167-7183.

Tyack, P.L. 2008. Implications for marine mammals of large-scale changes in the marine acoustic environment. *Journal of Mammalogy* 89(3): 549-558.

Warner, G., C. Erbe, and D. Hannay. 2010. Underwater Sound Measurements. (Chapter 3) *In* Reiser, C.M., D.W. Funk, R. Rodrigues, and D. Hannay (eds.). *Marine Mammal Monitoring and Mitigation during Open Water Shallow Hazards and Site Clearance Surveys by Shell Offshore Inc. in the Alaskan Chukchi Sea, July-October 2009: 90-Day Report*. LGL Report P1112-1. Report by LGL Alaska Research Associates Inc. and JASCO Applied Sciences for Shell Offshore Inc., National Marine Fisheries Service (US), and US Fish and Wildlife Service. 1-54.

Weilgart, L.S. 2007. The impacts of anthropogenic ocean noise on cetaceans and implications for management. *Canadian Journal of Zoology* 85: 1091-1116.

Wenz, G.M. 1962. Acoustic ambient noise in the ocean: Spectra and sources. *Journal of the Acoustical Society of America* 34(12): 1936-1956.

Wood, J., B.L. Southall, and D.J. Tollit. 2012. *PG&E offshore 3 D Seismic Survey Project EIR-Marine Mammal Technical Draft Report*. SMRU Ltd.

Zhang, Y. and C. Tindle. 1995. Improved equivalent fluid approximations for a low shear speed ocean bottom. *Journal of the Acoustical Society of America* 98(6): 3391-3396. http://scitation.aip.org/content/asa/journal/jasa/98/6/10.1121/1.413789.

Ziolkowski, A. 1970. A method for calculating the output pressure waveform from an air gun. *Geophysical Journal of the Royal Astronomical Society* 21(2): 137-161.

Zykov, M.M. 2016. *Modelling Underwater Sound Associated with Scotian Basin Exploration Drilling Project: Acoustic Modelling Report.* Document Number JASCO Document 01112, Version 2.0. Technical report by JASCO Applied Sciences for Stantec Consulting Ltd. http://www.ceaa.gc.ca/050/documents/p80109/116305E.pdf.

Appendix A. Underwater Acoustics

This section provides a detailed description of the acoustic metrics relevant to the modelling study and the modelling methodology.

A.1. Acoustic Metrics

Underwater sound pressure amplitude is measured in decibels (dB) relative to a fixed reference pressure of p_0 = 1 µPa. Because the perceived loudness of sound, especially pulsed noise such as from seismic airguns, pile driving, and sonar, is not generally proportional to the instantaneous acoustic pressure, several sound level metrics are commonly used to evaluate noise and its effects on marine life. We provide specific definitions of relevant metrics used in the accompanying report. Where possible we follow the ANSI and ISO standard definitions and symbols for sound metrics, but these standards are not always consistent.

The zero-to-peak sound pressure level, or peak pressure level (PK) ($L_{p,pk}$; dB re 1 µPa), is the maximum instantaneous sound pressure level in a stated frequency band attained by an acoustic pressure signal, $p(t)$:

$$L_{p,pk} = 20 \log_{10} \left[\frac{\max\left(\left| p(t) \right| \right)}{p_0} \right] . \qquad \text{(A-1)}$$

$L_{p,pk}$ is often included as a criterion for assessing whether a sound is potentially injurious; however, because it does not account for the duration of a noise event, it is generally a poor indicator of perceived loudness.

The sound pressure level (SPL) (L_p; dB re 1 µPa) is the root-mean-square (rms) pressure level in a stated frequency band over a specified time window (T, s) containing the acoustic event of interest. It is important to note that SPL always refers to an rms pressure level and therefore not instantaneous pressure:

$$L_p = 10 \log_{10} \left(\frac{1}{T} \int_T g(t)\, p^2(t) dt \Big/ p_0^2 \right) , \qquad \text{(A-2)}$$

where $g(t)$ is an optional time weighting function. The SPL represents a nominal effective continuous sound over the duration of an acoustic event, such as the emission of one acoustic pulse, a marine mammal vocalization, the passage of a vessel, or over a fixed duration. Because the window length, T, is the divisor, events with similar sound exposure level (SEL) but more spread out in time have a lower SPL.

In in-air studies of impulsive noise, the time weighting function $g(t)$ is often a decaying exponential that emphasizes more recent pressure signals to mimic the leaky integration of the mammalian hearing system. For example, human-based fast time weighting applies an exponential function with time constant 125 ms. Other approaches for evaluating L_p of impulsive signals include setting $g(t)$ to a boxcar (contant amplitude) function and T to the “90% time window” (T_{90}; the period over which cumulative square pressure function passes between 5% and 95% of its full per-pulse value) or to a constant value (e.g., T_{fix} = 125 ms).

The sound exposure level (SEL, dB re 1 µPa²·s) is a measure related to the acoustic energy contained in one or more acoustic events (*N*). The SEL for a single event is computed from the time-integral of the squared pressure over the full event duration (*T*):

$$L_E = 10\log_{10}\left(\int_T p^2(t)dt \Big/ T_0 p_0^2\right), \quad \text{(A-3)}$$

where T_0 is a reference time interval of 1 s. The SEL continues to increase with time when non-zero pressure signals are present. It therefore can be construed as a dose-type measurement, so the integration time used must be carefully considered in terms of relevance for impact to the exposed recipients.

SEL can be calculated over periods with multiple acoustic events or over a fixed duration. For a fixed duration, the square pressure is integrated over the duration of interest. For multiple events, the SEL can be computed by summing (in linear units) the SEL of the *N* individual events:

$$L_{E,N} = 10\log_{10}\left(\sum_{i=1}^{N} 10^{\frac{L_{E,i}}{10}}\right). \quad \text{(A-4)}$$

Because the SPL and SEL are both computed from the integral of square pressure, these metrics are related by the following expression, which depends only on the duration of the time window *T*:

$$L_p = L_E - 10\log_{10}(T). \quad \text{(A-5)}$$

Energy equivalent SPL (L_{eq}; dB re 1 µPa) denotes the SPL of a stationary (constant amplitude) sound that generates the same SEL as the signal being examined, $p(t)$, over the same period of time, *T*:

$$L_{eq} = 10\log_{10}\left(\frac{1}{T}\int_T p^2(t)dt \Big/ p_0^2\right). \quad \text{(A-6)}$$

The equations for SPL and the energy-equivalent SPL are numerically identical; conceptually, the difference between the two metrics is that the former is typically computed over short periods (typically of one second or less) and tracks the fluctuations of a non-steady acoustic signal, whereas the latter reflects the average SPL of an acoustic signal over times typically of one minute to several hours.

If applied, the frequency weighting of an acoustic event should be specified, as in the case of M-weighted SEL (e.g., $L_{E,LFC,24h}$; Appendix A.3).

A.1.1. 1/3-Octave-Band Analysis

The distribution of a sound's power with frequency is described by the sound's spectrum. The sound spectrum can be split into a series of adjacent frequency bands. Splitting a spectrum into 1 Hz wide bands, called passbands, yields the power spectral density of the sound. This splitting of the spectrum into passbands of a constant width of 1 Hz, however, does not represent how animals perceive sound.

Because animals perceive exponential increases in frequency rather than linear increases, analyzing a sound spectrum with passbands that increase exponentially in size better approximates real-world scenarios. In underwater acoustics, a spectrum is commonly split into 1/3-octave-bands, which are one-third of an octave wide; each octave represents a doubling in sound frequency. The centre frequency of the ith 1/3-octave-band, $f_c(i)$, is defined as:

$$f_c(i) = 10^{i/10} , \tag{A-7}$$

and the low (f_{lo}) and high (f_{hi}) frequency limits of the ith 1/3-octave-band are defined as:

$$f_{lo} = 10^{-1/20} f_c(i) \quad \text{and} \quad f_{hi} = 10^{1/20} f_c(i) . \tag{A-8}$$

The 1/3-octave-bands become wider with increasing frequency, and on a logarithmic scale the bands appear equally spaced (Figure A-1). The acoustic modelling spans from band 10 ($f_c(10)$ = 10 Hz) to band 44 ($f_c(44)$ = 25 kHz).

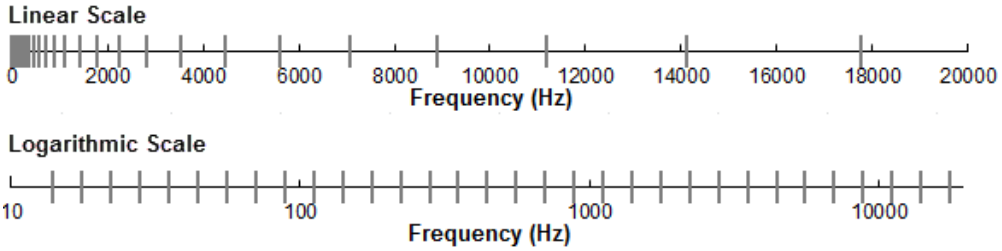

Figure A-1. One-third-octave-bands shown on a linear frequency scale and on a logarithmic scale.

The sound pressure level in the ith 1/3-octave-band $(L_b^{(i)})$ is computed from the power spectrum $S(f)$ between f_{lo} and f_{hi}:

$$L_b^{(i)} = 10 \log_{10} \left(\int_{f_{lo}}^{f_{hi}} S(f) df \right) , \tag{A-9}$$

Summing the sound pressure level of all the 1/3-octave-bands yields the broadband sound pressure level:

$$\text{Broadband SPL} = 10 \log_{10} \sum_i 10^{L_b^{(i)}/10} , \tag{A-10}$$

Figure A-2 shows an example of how the 1/3-octave-band sound pressure levels compare to the power spectrum of an ambient noise signal. Because the 1/3-octave-bands are wider with increasing frequency, the 1/3-octave-band SPL is higher than the power spectrum, especially at higher frequencies. Acoustic modelling of 1/3-octave-bands require less computation time than 1 Hz bands and still resolves the frequency-dependence of the sound source and the propagation environment.

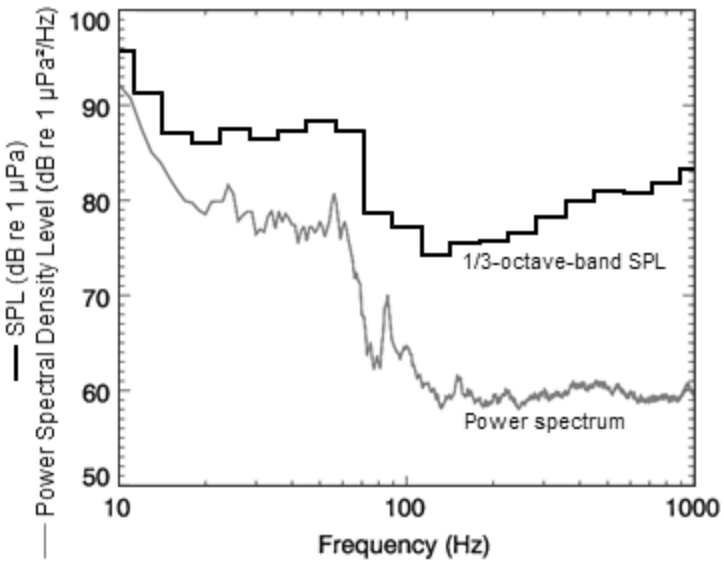

Figure A-2. A power spectrum and the corresponding 1/3-octave-band sound pressure levels of example ambient noise shown on a logarithmic frequency scale.

A.2. Marine Mammal Impact Criteria

It has been long recognized that marine mammals can be adversely affected by underwater anthropogenic noise. For example, Payne and Webb (1971) suggest that communication distances of fin whales are reduced by shipping sounds. Subsequently, similar concerns arose regarding effects of other underwater noise sources and the possibility that impulsive sources—primarily airguns used in seismic surveys—could cause auditory injury. This led to a series of workshops held in the late 1990s, conducted to address acoustic mitigation requirements for seismic surveys and other underwater noise sources (NMFS 1998, ONR 1998, Nedwell and Turnpenny 1998, HESS 1999, Ellison and Stein 1999). In the years since these early workshops, a variety of thresholds have been proposed for both injury (Appendix A.2.1) and disturbance (Appendix A.2.2). The following sections summarize the development of the current thresholds relevant to this study; this remains an active research topic, however.

A.2.1. Injury

The NMFS SPL criteria for injury to marine mammals from acoustic exposure were set according to recommendations for cautionary estimates of sound levels leading to onset of permanent hearing threshold shift (PTS). These criteria prescribed injury thresholds of 190 dB re 1 µPa SPL for pinnipeds and 180 dB re 1 µPa SPL for cetaceans, for all types of sound sources except tactical sonar and explosives (NMFS 2016). These injury thresholds are applied to individual noise pulses or instantaneous sound levels and do not consider the overall duration of the noise or its acoustic frequency distribution.

Criteria that do not account for exposure duration or noise spectra are generally insufficient on their own for assessing hearing injury. Human workplace noise assessment metrics consider the SPL as well as the duration of exposure and sound spectral characteristics. For example, the International Institute of Noise Control Engineering (I-INCE) and the Occupational Safety and Health Administration (OSHA) suggests thresholds in C-weighted peak pressure level and A-weighted time-average sound level (dB(A)[2] L_{eq}). They also suggest exchange rates that increase the allowable thresholds for each halving or doubling of exposure time. This approach assumes that hearing damage depends on the relative loudness perceived

[2] The “A” refers to a specific frequency-dependent filter shaped according to a human equal loudness contour.

by the human ear, and that the ear might partially recover from past exposures, particularly if there are periods of quiet nested within the overall exposure.

In recognition of shortcomings of the SPL-only based injury criteria, in 2005 NMFS sponsored the Noise Criteria Group to review literature on marine mammal hearing to propose new noise exposure criteria. Members of this expert group published a landmark paper (Southall et al. 2007) that suggested assessment methods similar to those applied for humans. The resulting recommendations introduced dual acoustic injury criteria for impulsive sounds that included peak pressure level thresholds and SEL_{24h} thresholds, where the subscripted 24h refers to the accumulation period for calculating SEL. The peak pressure level criterion is not frequency weighted whereas the SEL_{24h} is frequency weighted according to one of four marine mammal species hearing groups: Low-, Mid- and High-Frequency Cetaceans (LFC, MFC, and HFC respectively) and Pinnipeds in Water (PINN). These weighting functions are referred to as M-weighting filters (analogous to the A-weighting filter for human; Appendix A.3). The SEL_{24h} thresholds were obtained by extrapolating measurements of onset levels of Temporary Threshold Shift (TTS) in belugas by the amount of TTS required to produce Permanent Threshold Shift (PTS) in chinchillas. The Southall et al. (2007) recommendations do not specify an exchange rate, which suggests that the thresholds are the same regardless of the duration of exposure (i.e., it infers a 3 dB exchange rate).

Wood et al. (2012) refined Southall et al.'s (2007) thresholds, suggesting lower injury values for LFC and HFC while retaining the filter shapes (Appendix A.3). Their revised thresholds were based on TTS-onset levels in harbour porpoises from Lucke et al. (2009), which led to a revised impulsive sound PTS threshold for HFC of 179 dB re 1 $\mu Pa^2 \cdot s$. Because there were no data available for baleen whales, Wood et al. (2012) based their recommendations for LFC on results obtained from MFC studies. In particular they referenced Finneran and Schlundt (2010) research, which found mid-frequency cetaceans are more sensitive to non-impulsive sound exposure than Southall et al. (2007) assumed. Wood et al. (2012) thus, recommended a more conservative TTS-onset level for LFC of 192 dB re 1 $\mu Pa^2 \cdot s$.

Also in 2012, the US Navy recommended a different set of criteria for assessing Navy operations (Finneran and Jenkins 2012). Their analysis incorporated new dolphin equal-loudness contours[3] to update weighting functions and injury thresholds for LFC, MFC, and HFC. They recommended separating the pinniped group into otariids (eared seals) and phocids (earless seals) and assigning adjusted frequency thresholds to the former based on several sensitivity studies (Schusterman et al. 1972, Moore and Schusterman 1987, Babushina et al. 1991, Kastak and Schusterman 1998, Kastelein et al. 2005, Mulsow and Reichmuth 2007, Mulsow et al. 2011a, Mulsow et al. 2011b).

Although a definitive approach is not yet apparent, there is consensus in the research community that an SEL-based method is preferable either separately or in addition to an SPL-based approach to assess the potential for injuries. In August 2016, after substantial public and expert input into three draft versions and based largely on the above-mentioned literature (NOAA 2013, 2015, 2016), NMFS finalized and promulgated technical guidance for assessing the effect of anthropogenic sound on marine mammal hearing (NMFS 2016). The guidance describes injury criteria with new thresholds and frequency weighting functions for the five hearing groups described by Finneran and Jenkins (2012). Table A-1 provide the recommended thresholds.

[3] An equal-loudness contour is the measured sound pressure level (dB re 1 µPa for underwater sounds) over frequency, for which a listener perceives a constant loudness when exposed to pure tones.

Table A-1. Marine mammal injury (PTS onset) thresholds based on NMFS (2016).

Hearing group	Impulsive source		Non-impulsive source
	PK	Weighted SEL (24 h)	Weighted SEL (24 h)
Low-frequency cetaceans	219	183	199
Mid-frequency cetaceans	230	185	198
High-frequency cetaceans	202	155	173
Phocid pinnipeds in water	218	185	201
Otariid pinnipeds in water	232	203	219

A.2.2. Disturbance

The NMFS currently uses SPL thresholds for behavioural response of 160 dB re 1 µPa for impulsive sounds and 120 dB re 1 µPa for non-impulsive sounds for all marine mammal species (NMFS 2013), based on observations of mysticetes (Malme et al. 1983, Malme et al. 1984, Richardson et al. 1986, Richardson et al. 1990). As of 2016, NMFS applies these disturbance thresholds as a default, but makes exceptions on a species-specific and sub-population specific basis where warranted.

A.3. Marine Mammal Frequency Weighting

The potential for noise to affect animals depends on how well the animals can hear it. Noises are less likely to disturb or injure an animal if they are at frequencies that the animal cannot hear well. An exception occurs when the sound pressure is so high that it can physically injure an animal by non-auditory means (i.e., barotrauma). For sound levels below such extremes, the importance of sound components at particular frequencies can be scaled by frequency weighting relevant to an animal's sensitivity to those frequencies (Nedwell and Turnpenny 1998, Nedwell et al. 2007).

A.3.1. Marine Mammal Frequency Weighting Functions

In 2015, a U.S. Navy technical report by Finneran (2015) recommended new auditory weighting functions. The overall shape of the auditory weighting functions is similar to human A-weighting functions, which follows the sensitivity of the human ear at low sound levels. The new frequency-weighting function is expressed as:

$$G(f) = K + 10\log_{10}\left[\left(\frac{(f/f_{lo})^{2a}}{\left[1+(f/f_{lo})^{2}\right]^{a}\left[1+(f/f_{hi})^{2}\right]^{b}}\right)\right], \qquad \text{(A-11)}$$

Finneran (2015) proposed five functional hearing groups for marine mammals in water: low-, mid-, and high-frequency cetaceans, phocid pinnipeds, and otariid pinnipeds. The parameters for these frequency-weighting functions were further modified the following year (Finneran 2016) and were adopted in NOAA's technical guidance that assesses noise impacts on marine mammals (NMFS 2016). Table A-2 lists the frequency-weighting parameters for each hearing group; Figure A-3 shows the resulting frequency-weighting curves.

Table A-2. Parameters for the auditory weighting functions recommended by NMFS (2016).

Hearing group	*a*	*b*	f_{lo} (Hz)	f_{hi} (Hz)	*K* (dB)
Low-frequency cetaceans	1.0	2	200	19,000	0.13
Mid-frequency cetaceans	1.6	2	8,800	110,000	1.20
High-frequency cetaceans	1.8	2	12,000	140,000	1.36
Phocid pinnipeds in water	1.0	2	1,900	30,000	0.75
Otariid pinnipeds in water	2.0	2	940	25,000	0.64

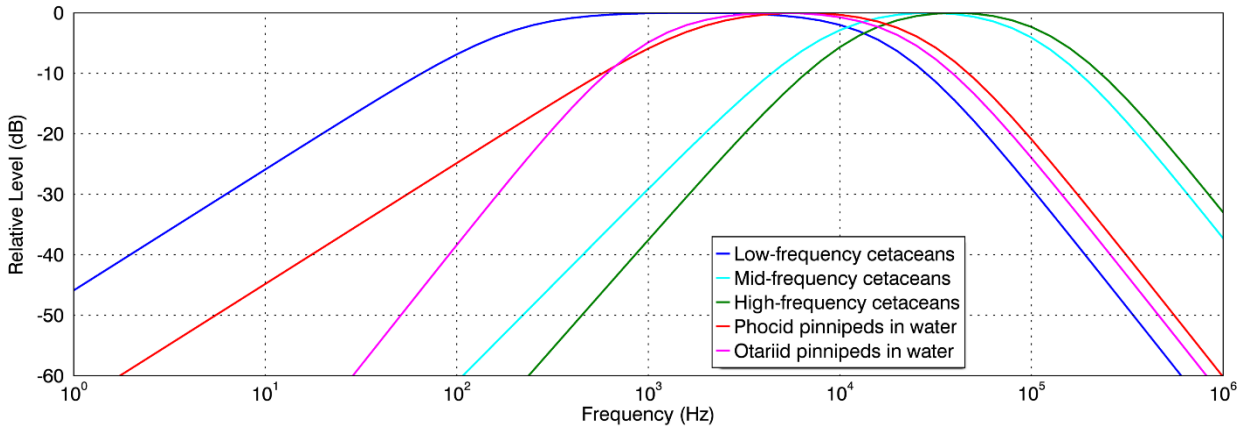

Figure A-3. Auditory weighting functions for functional marine mammal hearing groups as recommended by NMFS (2016).

A.4. Types of Sound

Numerous scientific reviews and workshops over the past 40 years have focused on how anthropogenic sounds can affect marine life (e.g., Payne and Webb 1971, Fletcher and Busnel 1978, Richardson et al. 1995, MMC 2007, Nowacek et al. 2007, Southall et al. 2007, Weilgart 2007, Tyack 2008). When assessing potential impacts of anthropogenic sound on marine life, sounds are commonly divided into two main categories: pulsed (with pulses further split into single and multiple pulses) and non-pulsed sounds (Southall et al. 2007).

Pulsed sounds include impact pile driving, airgun pulses, and some types of sonar. Non-pulsed sounds include vessel propulsion sound and some types of sonar. Numerous definitions and mathematical expressions (e.g., Burdic 1984) distinguish pulsed and non-pulsed sounds from one another.

A.4.1. Airgun Arrays

Seismic airguns generate pulsed acoustic energy by releasing a highly compressed air bubble into the water that expands and then collapses. Seismic airgun source arrays are comprised of multiple individual source elements, which are activated together to produce an output with frequencies ranging from several hertz to several kilohertz. Larger individual source element volumes producing lower frequencies and higher sound levels.

A single source element produces an approximately omnidirectional sound field, emitting acoustic energy equally in all directions. Multiple element seismic source arrays exhibit directivity due to geometric separation of the elements. The geometric separation translates into phase shift during the superposition of acoustic waves emitted by individual elements. The phase shift depends not only on the value of the geometrical separation, but also on the frequency. The effect of the superposition can be constructive or

destructive. For VSP surveys, source array layouts are configured to achieve higher sound energy emission levels in the vertical direction where at far-field the pulses from all elements add in-phase, since there is virtually no geometric shift along the z-axis for the array elements. Lower levels of sound energy are emitted in other directions. Airgun source arrays might show significant directionality in the horizontal direction due to the phase delay between pulses because the elements are horizontally separated. The directivity pattern of an airgun source array is different at different frequencies.

A.4.2. Vessel Sounds

Underwater sound that radiates from vessels is produced mainly by propeller and thruster cavitation, with a smaller fraction of sound produced by sound transmitted through the hull, such as by engines, gearing, and other mechanical systems. Sound levels tend to be the highest when thrusters are used to position the vessel and when the vessel is transiting at high speeds. A vessel's sound signature depends on the vessel's size, power output, propulsion system, and the design characteristics of the given system (e.g., blade shape and size). A vessel produces broadband acoustic energy with most of the energy emitted below a few kilohertz. Sound from onboard machinery, particularly sound below 200 hertz (Hz), dominates the sound spectrum before cavitation begins—normally around 8–12 knots on many commercial vessels (Spence et al. 2007). Under higher speeds and higher propulsion system load, the acoustic output from the cavitation processes on the propeller blades dominates other sources of sound on the vessel (Leggat et al. 1981).

A.5. Source Models

A.5.1. AASM

The source levels and directivity of the airgun array were predicted with JASCO's Airgun Array Source Model (AASM; MacGillivray 2006). AASM includes both a low-frequency and a high-frequency module for predicting different components of the airgun array spectrum. The low frequency module is based on the physics of oscillation and radiation of airgun bubbles, as originally described by Ziolkowski (1970), that solves the set of parallel differential equations that govern bubble oscillations. Physical effects accounted for in the simulation include pressure interactions between airguns, port throttling, bubble damping, and generator-injector (GI) gun behaviour discussed by Dragoset (1984), Laws et al. (1990), and Landro (1992). A global optimization algorithm tunes free parameters in the model to a large library of airgun source signatures.

While airgun signatures are highly repeatable at the low frequencies, which are used for seismic imaging, their sound emissions have a large random component at higher frequencies that cannot be predicted deterministically. Therefore, the high-frequency module of AASM uses a stochastic simulation to predict the sound emissions of individual airguns above 800 Hz, using a multivariate statistical model. The current version of AASM has been tuned to fit a large library of high quality seismic source signature data obtained from the Joint Industry Program (JIP) on Sound and Marine Life (Mattsson and Jenkerson 2008). The stochastic model uses a Monte-Carlo method to simulate the random component of the high-frequency spectrum of each airgun in an array. The mean high-frequency spectra from the stochastic model augment the low-frequency signatures from the physical model, allowing AASM to predict airgun source levels at frequencies up to 25,000 Hz.

AASM produces a set of notional signatures for each array element based on:

- Array layout
- Volume, tow depth, and firing pressure of each airgun
- Interactions between different airguns in the array

These notional signatures are the pressure waveforms of the individual airguns at a standard reference distance of 1 m; they account for the interactions with the other airguns in the array. The signatures are

summed with the appropriate phase delays to obtain the far-field source signature of the entire array in all directions. This far-field array signature is filtered into 1/3-octave-bands to compute the source levels of the array as a function of frequency band and azimuthal angle in the horizontal plane (at the source depth), after which it is considered to be a directional point source in the far field.

A seismic array consists of many sources and the point-source assumption is invalid in the near field where the array elements add incoherently. The maximum extent of the near field of an array (R_{nf}) is:

$$R_{\mathrm{nf}} < \frac{l^2}{4\lambda} , \tag{A-12}$$

where λ is the sound wavelength and l is the longest dimension of the array (Lurton 2002, §5.2.4). For example, an airgun array length of l = 16 m yields a near-field range of 85 m at 2 kHz and 17 m at 100 Hz. Beyond this R_{nf} range, the array is assumed to radiate like a directional point source and is treated as such for propagation modelling.

The interactions between individual elements of the array create directionality in the overall acoustic emission. Generally, this directionality is prominent mainly at frequencies in the mid-range between tens of hertz to several hundred hertz. At lower frequencies, with acoustic wavelengths much larger than the inter-airgun separation distances, the directionality is small. At higher frequencies, the pattern of lobes is too finely spaced to be resolved and the effective directivity is less.

A.5.2. Vessels

Most vessels have two primary sound sources: the machinery and the propellers/thrusters. For vessels operating in the heavily loaded conditions (e.g., during acceleration, dynamic positioning in heavy weather, or with heavy load), the underwater sound generated by the cavitation processes on the propeller blades dominates the sound field form the vessel (Leggat et al. 1981). Based on an analysis of acoustic recordings of merchant vessels, Ross (1976) showed that the sound intensity from the propellers is proportional to the number of blades, the propeller diameter, and the propeller tip speed. Ross (1976) provided the following formula for the sound levels from a vessel's propeller, operating in calm, open ocean conditions:

$$L_{100} = 155 + 60\log(u/25) + 10\log(B/4) , \tag{A-13}$$

where L_{100} is the spectrum level at 100 Hz, u is the propeller tip speed (m/s), and B is the number of propeller blades. Equation A-13 estimates the broadband SPL produced by the propeller cavitation at frequencies between 100 Hz and 10 kHz. This equation is valid for a propeller tip speed between 15 and 50 m/s. The spectrum is assumed to be flat below 100 Hz, and falls off at a rate of −6 dB per octave above 100 Hz (Figure A-4).

Another method of predicting the source level of a propeller was suggested by Brown (1977). For propellers operating in heavily loaded conditions, the formula for the sound spectrum level is:

$$\mathrm{SL}_B = 163 + 40\log D + 30\log N + 10\log B - 20\log f + 10\log(A_c/A_D) , \tag{A-14}$$

where D is the propeller diameter (m), N is the propeller revolution rate per second, B is the number of blades, A_C is the area of the blades covered by cavitation, and A_D is the total propeller disc area. Similar to Ross's approach, the spectrum below 100 Hz is assumed to be flat. The tests with a naval propeller operating at off-design heavily loaded conditions showed that Equation A-14 should be used with a value of $A_c/A_D = 1$ (Leggat et al. 1981).

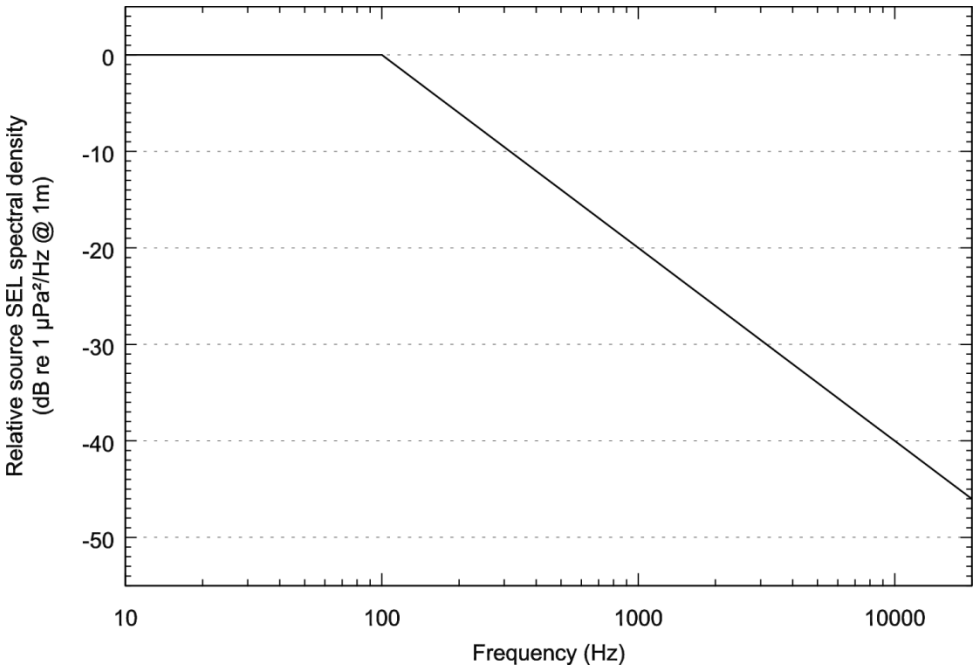

Figure A-4. Estimated sound spectrum from cavitating propeller (Leggat et al. 1981).

A.6. Sound Propagation Models

A.6.1. Transmission Loss

The propagation of sound through the environment was modelled by predicting the acoustic transmission loss—a measure, in decibels, of the decrease in sound level between a source and a receiver some distance away. Geometric spreading of acoustic waves is the predominant way by which transmission loss occurs. Transmission loss also happens when the sound is absorbed and scattered by the seawater, and absorbed scattered, and reflected at the water surface and within the seabed. Transmission loss depends on the acoustic properties of the ocean and seabed; its value changes with frequency.

If the acoustic source level (SL), expressed in dB re 1 µPa @ 1 m or dB re 1 µPa^2·s @ 1 m, and transmission loss (TL), in units of dB, at a given frequency are known, then the received level (RL) at a receiver location can be calculated in dB re 1 µPa @ 1 m by:

$$RL = SL - TL \, . \qquad \text{(A-15)}$$

A.6.2. Noise Propagation with MONM and BELLHOP

Underwater sound propagation (i.e., transmission loss) at frequencies of 10 Hz to 25 kHz was predicted with JASCO's Marine Operations Noise Model (MONM) and BELLHOP. The models compute received per-pulse SEL for directional impulsive sources, and SEL over 1 s for non-impulsive sources, at a specified source depth.

MONM computes acoustic propagation at low frequency (below 1 kHz for the present study) via a wide-angle parabolic equation solution to the acoustic wave equation (Collins 1993) based on a version of the U.S. Naval Research Laboratory's Range-dependent Acoustic Model (RAM), which has been modified to account for a solid seabed (Zhang and Tindle 1995). The parabolic equation method has been extensively benchmarked and is widely employed in the underwater acoustics community (Collins et al. 1996). MONM computes acoustic propagation at high frequency (below 2–25 kHz) via the BELLHOP

Gaussian beam acoustic ray-trace model (Porter and Liu 1994). This version of MONM accounts for sound attenuation due to energy absorption through ion relaxation and viscosity of water in addition to acoustic attenuation due to reflection at the medium boundaries and internal layers (Fisher and Simmons 1977). The former type of sound attenuation is significant for frequencies higher than 5 kHz and cannot be neglected without noticeably affecting the model results. MONM's predictions have been validated against experimental data from several underwater acoustic measurement programs conducted by JASCO (Hannay and Racca 2005, Aerts et al. 2008, Funk et al. 2008, Ireland et al. 2009, O'Neill et al. 2010, Warner et al. 2010, Racca et al. 2012a, Racca et al. 2012b, Martin et al. 2015).

MONM accounts for the additional reflection loss at the seabed, which results from partial conversion of incident compressional waves to shear waves at the seabed and sub-bottom interfaces, and it includes wave attenuations in all layers. MONM incorporates the following site-specific environmental properties: a bathymetric grid of the modelled area, underwater sound speed as a function of depth, and a geoacoustic profile based on the overall stratified composition of the seafloor.

MONM computes acoustic fields in three dimensions by modelling transmission loss within two-dimensional (2-D) vertical planes aligned along radials covering a 360° swath from the source, an approach commonly referred to as N×2-D. These vertical radial planes are separated by an angular step size of $\Delta\theta$, yielding N = 360°/$\Delta\theta$ number of planes (Figure A-5).

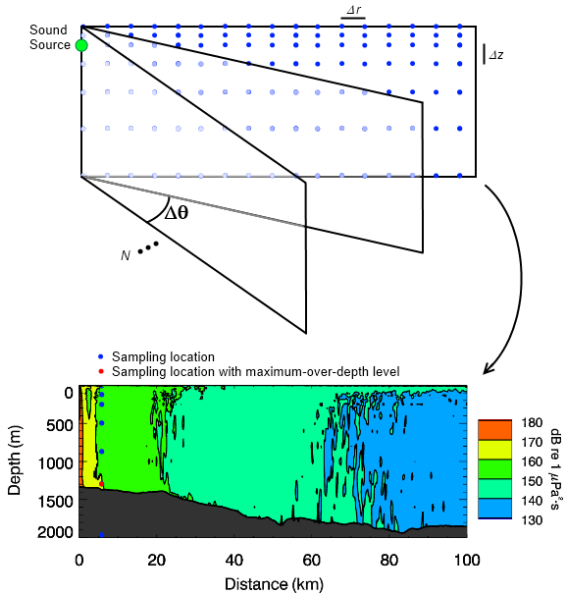

Figure A-5. The N×2-D and maximum-over-depth modelling approach used by MONM.

MONM treats frequency dependence by computing acoustic transmission loss at the centre frequencies of 1/3-octave-bands. Sufficiently many 1/3-octave-bands, starting at 10 Hz, are modelled to include the majority of acoustic energy emitted by the source. At each centre frequency, the transmission loss is modelled within each of the N vertical planes as a function of depth and range from the source. The 1/3-octave-band received per-pulse SELs are computed by subtracting the band transmission loss values from the directional source level in that frequency band. Composite broadband received SELs are then computed by summing the received 1/3-octave-band levels.

The received per-pulse SEL sound field within each vertical radial plane is sampled at various ranges from the source, generally with a fixed radial step size. At each sampling range along the surface, the sound field is sampled at various depths, with the step size between samples increasing with depth below the surface. The step sizes are chosen to provide increased coverage near the depth of the source and at depths of interest in terms of the sound speed profile. For areas with deep water, sampling is not performed at depths beyond those reachable by marine mammals. The received per-pulse SEL at a surface sampling location is taken as the maximum value that occurs over all samples within the water

column, i.e., the maximum-over-depth received per-pulse SEL. These maximum-over-depth per-pulse SELs are presented as colour contours around the source (Figure A-6).

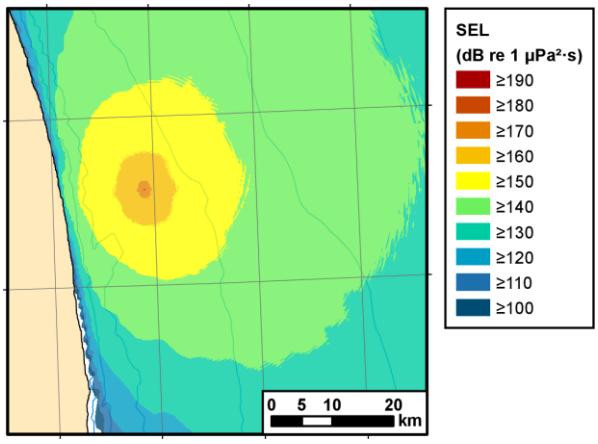

Figure A-6. Example of a maximum-over-depth SEL colour contour map for an unspecified source.

A.6.3. Noise Propagation with FWRAM

For impulsive sounds, time-domain representations of the pressure waves generated in the water are required to calculate SPL and peak pressure level. For this study, synthetic pressure waveforms were computed using FWRAM, which is a time-domain acoustic model based on the same wide-angle parabolic equation (PE) algorithm as MONM. FWRAM computes synthetic pressure waveforms versus range and depth for range-varying marine acoustic environments, and it takes the same environmental inputs as MONM (bathymetry, water sound speed profile, and seabed geoacoustic profile). Unlike MONM, FWRAM computes pressure waveforms via Fourier synthesis of the modelled acoustic transfer function in closely spaced frequency bands. FWRAM employs the array starter method to accurately model sound propagation from a spatially distributed source (MacGillivray and Chapman 2012).

Synthetic pressure waveforms were modelled over the frequency range 10–2048 Hz, inside a 1 s window (Figure A-7). The synthetic pressure waveforms were post-processed, after applying a travel time correction, to calculate standard SPL and SEL metrics versus range and depth from the source.

Besides providing direct calculations of the peak pressure level and SPL, the synthetic waveforms from FWRAM can also be used to convert the SEL values from MONM to SPL.

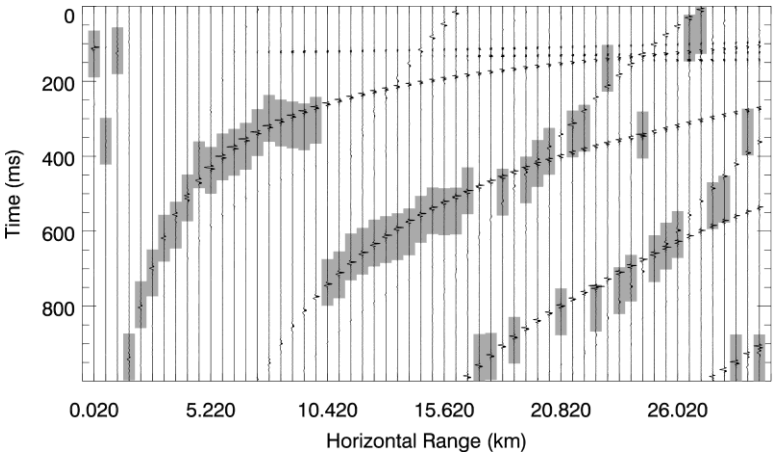

Figure A-7. Example of synthetic pressure waveforms computed by FWRAM for at the VSP airgun array multiple range offsets. Receiver depth is 2 m and the amplitudes of the pressure traces have been normalised for display purposes.